Placental transfer of xenobiotics in pregnancy physiologically-based pharmacokinetic models: Structure and data

Marc Codaccioni, Frédéric Bois, Céline Brochot

Placental transfer of xenobiotics in pregnancy physiologically-based pharmacokinetic models: structure and data

Marc Codaccioni[*], Frédéric Bois[*1], Céline Brochot[*ǂ].

*Models for Ecotoxicology and Toxicology unit (DRC/VIVA/METO), Institut National de l'Environnement Industriel et des Risques, 60550 Verneuil-en-Halatte, France.

ǂ Corresponding author; Tel: +333 44 55 68 50; e-mail: celine.brochot@ineris.fr

[1] Frederic. Y. Bois is currently employed at CERTARA, Simcyp division, Sheffield S2 4SU, United Kingdom.

1 INTRODUCTION

Numerous chemical substances, whether endogenous or exogenous, can cross the placental barrier and reach the fetal bloodstream and organs [1]. Prenatal exposures to harmful xenobiotics can lead to developmental toxicities with future health consequences for the life of the growing child [2, 3]. It is extremely likely that the intensity and nature of the effects are dependent on the window of exposure to xenobiotics during prenatal life [4]. Fetal internal exposure, defined as the amount of xenobiotic or its metabolites in developing organs or fetal blood, is a key factor of the risk of toxic effects. For ethical reasons, human fetal blood sampling during gestation is not an option. Maternal concentrations during pregnancy and cord blood concentrations at delivery can be used to estimate fetal internal exposure over pregnancy or at term [5]. However, in the absence of precise information on the mother's environmental exposures (doses, times of exposure *etc*.), this kind of data can be difficult to interpret [6].

In silico models become relevant for estimating the internal fetal exposure to chemicals during pregnancy using indirect or incomplete data. Pregnancy physiologically-based pharmacokinetic (pPBPK) models can simulate internal exposures of different maternal and fetal organs to a specific substance [7]. These models aim to predict chemicals fate in the body by a system of mass balance differential equations describing absorption, distribution, metabolism and elimination (ADME) mechanisms. They represent the maternal and fetal bodies as a set of compartments corresponding to tissues or organs [8]. Mass transfers between compartments follow physiological blood flows and potential diffusions. However, pregnancy is not a static condition. Many structural and physiological changes occur in the mother to ensure the development of the fetus: increase of volumes and blood flows, induction or inhibition of metabolic enzymes *etc.* (Figure 1) [9, 10]. These changes impact the maternal internal exposure to a chemical which differs from non-pregnant women [11] and can show

large differences between the three trimesters of pregnancy [12]. In pPBPK modeling, tissue volumes, blood flows and other parameters which change throughout pregnancy are usually defined as time-dependent variables [13]. Although fetal internal exposures are dependent on the ADME processes which occur in the mother and fetus, placental transfer contribution is a critical point that can be supported by the extrapolation of transplacental transfer quantitative data from non-*in vivo* human based approaches (*e.g., in silico*, *in vitro*, *ex vivo* or animal *in vivo* data) [14].

This review focuses on the various placental transfer models developed in animal and human pPBPK models and the experimental methods currently available to quantify placental transfer rates. The first section summarizes the evolution of the physiology and anatomy of the placenta during pregnancy and identifies the key parameters of transplacental transfers. The second section reviews the pPBPK structures for placental transfers and assesses the influence of the modeling structure on the estimation of the fetal exposure using model simulations. The last part presents computational and experimental methods and data that can be used to quantify the rate of placental transfers in pPBPK models.

2 PLACENTAL TRANSFER ANATOMICAL AND PHYSIOLOGICAL KEY POINTS

2.1 STRUCTURE OF THE HUMAN PLACENTA

The placenta is a disc-shaped organ which forms the interface between the mother and the fetus [15]. It ensures several functions which include gas and waste products materno-fetal exchange, hormonal secretion and transfer of immunity [16]. The placenta originates from the early trophoblastic invasion of the maternal uterine mucosa and its vascular re-shaping [17]. The trophoblastic incursion gives rise to the intervillous space. The latter physically separates two poles: the chorionic plate at the fetal side and the basal plate in contact with the maternal

decidua. Vascular projections surrounded by mesenchymal tissues and an external trophoblast layer grow up from the chorionic plate and form chorionic villi. The later are lumped on trunk structures which bath into maternal blood in the intervillous space (Figure 2A). Those structural units are called cotyledons. At term, the number of villous tree structures is between fifteen and thirty [18]. The villus inner part contains stroma cells and fetal blood vessels which arise from the extraembryonic mesoderm, while the surrounding trophoblast is composed by a double layer of inner cytotrophoblasts and outer syncytiotrophoblasts (Figure 2B). Mononucleated cytotrophoblasts are the precursors of the multinucleated syncytiotrophoblast layer. The latter play a crucial endocrine role, producing proteins and steroid hormones such as human chorionic gonadotropin (hCG), human placental lactogen, pregnancy-specific glycoprotein and leptin [19, 20].

The placenta is perfused both by maternal and fetal blood, which never mix. The trophoblastic uterine invasion during the first trimester of gestation leads to the growth of maternal blood vessels up to the point of implantation and their dilation [21]. The vascular remodeling generates the confluence of the uterine and ovarian arteries which forms the arcuate arteries [22]. They supply newly formed spiral arteries in the endometrium. At the end of the first trimester, the spiral arteries provide maternal incoming blood flow to the intervillous space. On the fetal side, the villi are supplied with deoxygenated blood through the chorionic arteries, deriving from two umbilical arteries, and which branch in a centrifugal pattern into their final branches [23]. The chorionic veins merge into a single umbilical vein which contains oxygenated fetal blood (Figure 2A).

The materno-fetal blood interface is a three-layers structure (Figure 2B & 2C), which consists of the endothelium of fetal capillaries, the surrounding mesenchyme (connective tissue with Hoffbauer cells and fibroblasts) and the trophoblast (continuous syncytiotrophoblast with cytotrophoblasts underneath). The cytotrophoblast population decreases significantly as villi

mature, so much that, at term, the cytotrophoblast layer becomes lacunary [22] (Figure 2C). The distance between maternal and fetal blood thins out during pregnancy from 50 µm at the late second month to less than 5 µm by the 37th week of gestation [24]. Placental volume and the number of chorionic villi and branches increase all along gestation so that the materno-fetal exchange surface reaches almost 15 m^2 [25].

2.2 PLACENTAL TRANSFER OF XENOBIOTICS

During the first trimester, chemicals and nutrients can reach the embryo by phagocytosis of extracellular material from the eroded endometrium and uterine glands (histiotrophic nutrition) and the diffusion from maternal endometrial microcirculation (hemotrophic nutrition) [26]. This primitive utero-placental microcirculation (an immature intervillous space) is structured with the syncytiotrophoblast lacunar network (observed by the second week of gestation) derived from the invasion of endometrial arterioles and the tertiary chorionic villous which contained fetal capillaries (observed by the third week of gestation) [17]. As soon as the spiral arteries are no longer plugged by trophoblast cells and a significant maternal blood flow is detectable within the placenta around the 12th week of gestation [26], the materno-fetal exchange between the maternal blood in the intervillous space and the capillaries of the chorionic villi becomes predominantly hemotrophic.

The transfer of substances between the maternal to fetal bloodstream comprises two major steps: materno- and feto-syncytiotrophoblast exchanges at the apical and basal face of the syncytiotrophoblast, respectively [27]. Placental transfers mechanisms include passive diffusion, active transport, facilitated diffusion, pinocytosis and phagocytosis [28]. Passive diffusion and active uptake/efflux, to a lesser extent, are the predominant mechanisms of placental transfer for small molecules [29]. Passive diffusion is the transfer of a chemical driven by a concentration gradient and does not need a source of energy. According to Fick's law, the transfer rate (amount of substance transferred per unit of time) depends on permeability,

thickness of the membrane and surface of exchange. Active transport is characterized by the transfer of chemicals against a concentration gradient. Because transporters capacity is limited, transfer mechanism can be saturated. A transporter can accept several substrates, which could lead to competition between them. Different types of efflux and influx proteins have been detected in the placenta at the apical (maternal facing brush border membrane) or basolateral (fetal facing basal membrane) sides of the syncytiotrophoblast cell layer [30]. For instance, some ATP-binding cassette (ABC) transporters (including the multidrug resistance protein 1, P-gp, and the multidrug resistance-associated proteins) are located at the apical surface of the syncytiotrophoblast ensuring the efflux of substances back to maternal circulation [31]. Depending on the localization and function, transporters may either increase or decrease xenobiotic transfer towards fetal circulation. Furthermore, cells of fetal capillaries hold transporters [14].

Passive diffusion is strongly affected by xenobiotics' physicochemical properties, such as the molecular weight (MW), the pKa for ionization, the lipid solubility, and the number of hydrogen bonding sites [32]. Chemicals which have a relatively low MW, a lipophilic profile and few hydrogen binding sites seem to diffuse more easily. Only molecules not bound to proteins can cross the placental barrier. Thus, the extent of protein binding occurring on both sides of the barrier may affect passive diffusion [33]. Albumin and α1-acid glycoprotein concentrations, which are the main plasmatic binding proteins, evolve during gestation in opposite manners for the mother and the fetus [34]. On the maternal side, plasma volume increases largely without a corresponding increase in plasma protein amounts, which leads to the dilution of blood proteins. On the fetus side, plasma proteins are secreted intensively and compensate the increase in plasma volume. Furthermore, fetal blood pH is lower in comparison to the maternal one. This leads to ionization and trapping of weak bases in the fetus [35] and conversely a relative trapping of weak acids on the maternal side. Some other parameters can

exert influence directly or indirectly on transfer through the placenta. Hypotension related to a pathologic condition or cotreatment may affect the utero-placental blood flow through the release of biogenic amines [27], since there is no autoregulation of the uteroplacental circulation [22]. After substances have entered the syncytiotrophoblast cytosol, they may be metabolized. Numerous studies have demonstrated the presence of xenobiotic-metabolizing enzymes in the placental tissue [18, 28]. This can lead to reduced transfer of parent chemicals to the fetus and to increase fetal exposure to metabolites.

3 pPBPK MODELS

We reviewed the pPBPK models published in the scientific literature and focused on the various model structures used to describe placental transfers. We searched PubMed using the queries “Pregnancy AND PBPK” (98 hits), “Placental transfer AND PBPK” (13 hits) in the titles, abstracts or keywords of articles. We also searched the Toxnet Developmental and Reproductive Toxicology Database (https://toxnet.nlm.nih.gov/newtoxnet/dart.htm) using the request “PBPK” (105 hits). That yielded a total of 216 results. We also used our focused reading list of published articles. From those searches, we keep out one of the papers that used the same model published, and leave out review papers [13], models which included the placenta and fetuses in a richly perfused organs compartment [36, 37], and insufficiently documented models in terms of placental transfer parameterization [38, 39]. That led us to select 50 publications presenting original pPBPK models. In the following, we present the transplacental transfer model structures, the parameterization of placental diffusion and physiological placental parameters (volume and blood flow), and the partitioning of substances between blood and placenta.

3.1 TRANSPLACENTAL TRANSFER MODEL STRUCTURES

We classified the selected 50 pPBPK models according to their placental transfer structure and gathered descriptive statistics on the use of those classes to document current practices in the field. We assigned models' structures to two groups: group 1 comprises models with a fetal PBPK sub-model (*i.e.,* at least one fetal compartment inflowed by fetal blood circulation); group 2 includes the others without a fetal sub-model.

In group 1, we identified eight placental transfer structures (Figure 3). The models differ in their description of placental-fetal exchanges, notably by the number and layout of placental sub-compartments. Only one class of models considers placental transfer as a perfusion-limited process (tissue membranes present no barriers to diffusion). In the other 7 classes, the distribution to placental sub-compartments involves a diffusion-limited process (diffusion across tissue membranes is slower than perfusion).

A general equation of the change in amount of the maternal placental compartment would be:

$$\frac{dQ_p}{dt} = F_{mat} \times \left(\frac{C_{maternalPBPK}}{PC_{maternalPBPK_{t:b}}} - \frac{C_p}{PC_{p_{t:b}}} \right) - transfer_{diffusion} \quad \text{(E1)}$$

where Q_p is the substance amount in placental tissue compartment expressed in [m] ([m] stands for mass), F_{mat} the inflowing maternal blood flow to the placental tissues expressed in [v].[t]$^{-1}$ ([v] and [t] stand for volume and time, respectively), $C_{maternalPBPK}$ the maternal tissue compartment concentration expressed in [m].[v]$^{-1}$, $PC_{maternalPBPK_{t:b}}$ the maternal tissue to blood partition coefficient, C_p the placental tissue compartment concentration expressed in [m].[v]$^{-1}$ and $PC_{pt:b}$ the placental tissue to blood partition coefficient. The generic diffusional exchange term ($transfer_{diffusion}$) depends on the modeling assumptions detailed below. For instance, the exchange term in Lumen et al. [40] is set between the placental tissue and a maternal placental blood compartment as follow:

$$transfer_{diffusion} = K_{diffusion} \times (C_{mpb} - \frac{C_p}{PC_{p_{t:b}}}) \quad \text{(E2)}$$

$$K_{diffusion} = PAC \times BW_{fetal}^{0.75} \quad \text{(E3)}$$

where C_{mpb} and C_p refer to the maternal placental blood and the placental tissue concentrations, respectively, expressed in $[m].[v]^{-1}$, $PC_{pt:b}$ the placental tissue to blood partition coefficient. $K_{diffusion}$ denotes the diffusional constant expressed in $[v].[t]^{-1}$. Again, the way of writing $K_{diffusion}$ varies between pPBPK models and several examples found in the literature are provided as Supplemental Material. In this example, Lumen et al. used a permeability surface area constant (PAC) expressed in $[v].[t]^{-1}.[m]^{-1}$ scaled to the fetal bodyweight (BW_{fetal}).

When the blood flow, rather than diffusion, is the limiting factor of placental transfer [41-43], the rate of change in placenta can be computed with the blood flow rate as proposed by Krishnan et al. [44]:

$$\frac{dQ_p}{dt} = F_{mat} \times \frac{C_{maternalPBPK}}{PC_{maternalPBPK_{t:b}}} + F_{fet} \times \frac{C_{fetalPBPK}}{PC_{fetalPBPK_{t:b}}} - (F_{mat} + F_{fet}) \times \frac{C_p}{PC_{p_{t:b}}} \quad \text{(E4)}$$

where Q_p is the substance amount in placenta expressed in $[m]$, F_{mat} the inflowing maternal blood flow to the placenta expressed in $[v].[t]^{-1}$, $C_{maternalPBPK}$ the maternal tissue compartment concentration expressed in $[m].[v]^{-1}$, $PC_{maternalPBPKt:b}$ the maternal tissue to blood partition coefficient, F_{fet} the inflowing fetal blood to the placenta expressed in $[v].[t]^{-1}$, $C_{fetalPBPK}$ the fetal tissue compartment concentration expressed in $[m].[v]^{-1}$, $PC_{fetalPBPKt:b}$ the fetal tissue to blood partition coefficient, C_p the placental compartment concentration expressed in $[m].[v]^{-1}$ and $PC_{pt:b}$ the placental tissue to blood partition coefficient. The equations for the placental transfers of the eight classes of group 1 are given in Supplemental Material.

The models included in group 2 (no fetal sub-model) were developed to assess the impact of gestation on maternal dosimetry rather than to investigate fetal exposure. We identified four different placental transfer structures in this case that are presented Figure 4. In class I, the fetus is lumped in a fetoplacental unit with all the anatomical structures related to gestation (amniotic

fluid, placenta, uterus, fetus etc.) (*e.g.,* Gaohua, Abduljalil [45]), and the distribution of substances is perfusion-limited. In class J, the distribution between the fetus and the placenta or the uterus compartments is governed by simple diffusion (*e.g.,* Crowell, Sharma [46]). In K and L classes, a three-compartment structure is used for placental transfers. Class K distinguishes placental blood, placental tissue and fetal blood [47]; and class L differentiates placental blood, placental tissue and the fetus [48]. The equations for the different placental transfer structures of classes I, J, K and L are given in Supplemental Material.

Tables 1 and 2 sum up the placental transfer structures' classes models for the group 1 and 2, respectively. They also give a focus on the diffusion apparent transfer constant parameterizations, notably with the sources of data. Those parameters are in dimension of $[v].[t]^{-1}$, expressed either as a permeability times a surface area (*e.g.,* Martin, Oshiro [49]) or as a clearance (*e.g.,* Lin, Fisher [50]). Diffusion apparent parameters can be allometrically scaled to fetal or maternal body mass or they can be made proportional to the syncytiotrophoblast surface or to the placental weight to reflect the increase of placental transfer rate throughout gestation. Table 1 and Table 2 also provide information on the symmetry of transfer values between both directions. About half models assumed that the diffusional processes were symmetrical between maternal to fetal and fetal to maternal exchanges. Asymmetric parameterization is feasible when animal *in vivo* [52] or human placental *ex vivo* data [62] on xenobiotic transfer are available. In a human model for persistent compounds, Loccisano et al. also recalibrated the diffusional transfer constant with maternal and fetal blood levels observed in biomonitoring studies and found asymmetric values in materno-fetal exchanges [51].

Figure 5 presents the repartition of the models among the different classes. The most largely used structures belong to class D with 12 publications and to class J with 19 publications for group 1 and group 2, respectively. The other structure classes are most of the time used just once. Among the 50 models identified, 29 articles were developed for human (Table 1 and

Table 2). The others were developed for mice, rats or rabbits and 9 publications present both animal and human models. Figure 6A suggests that there is no clear pattern in the placental transfer structure according to species. The same conclusion is reached when the structure is examined according to the type of substances studied (Figure 6B), according to the symmetry or the asymmetry of the placental diffusional transfer parameters between mother and fetus (Figure 6C), or according to the source of information for the placental diffusional transfer parameterization (Figure 6D). This conclusion must, however, be qualified, given the low number of models and the fact that D and J classes are predominant.

To study the influence of the placental transfer structure on the maternal and fetal internal doses, we encoded the group 1 and group 2 placental transfer structures (as an example, Class B model is given as Supplementary Material) in GNU MCSim [52] (available at http://www.gnu.org/software/mcsim/). For each model structure, we simulated the same exposure scenario to a hypothetical substance. The exposure scenario and the models' parameterizations are given as Supplemental Material (Table S1). No elimination was included in the maternal nor fetal sub-models to focus on the placental transfer process. Every placental diffusion transfer constant was set to the arbitrary value of 1 $[v].[t]^{-1}$ to ensure structures comparability. Furthermore, no active placental uptake/efflux was included in addition to diffusion, as observed in the majority of the reviewed models. The maternal and fetal blood flows to placenta were set at 45 $[v].[t]^{-1}$ and 30 $[v].[t]^{-1}$ respectively. Figure 7A presents the fetal toxicokinetic profiles obtained for each class of group 1 and group 2. We identified four subgroups of transfer according to the time needed to reach an approximate steady-state. That delay increased with the number of diffusion constants between maternal and fetal blood circulations. For instance, the simulated fetal concentrations in B and C classes models (which have two diffusion constants between maternal and fetal blood circulations) reach steady-state in about 340 hours, whereas it takes about 180 hours for models belonging to A, D, E and G

252 classes (which all have one diffusion constant between maternal and fetal blood circulations).
253 The simulated fetal steady-state concentration for the G class model is higher than the other
254 classes because of its lowest total volume (which the sum of volumes of every maternal and
255 fetal compartment) owing to its structure (Table S1). The time to reach steady-state is
256 approximately 120 hours for the F class model. Based on our results, it should be close to 180
257 hours considering that it comprises a unique diffusion transfer constant between maternal and
258 fetal blood circulations. That difference between the F and A, D, E and G classes might be due
259 to the fact that diffusion is modelled between the tissular sub-compartments in the first case and
260 between blood compartments or blood and tissue compartments in the second case. It should
261 be noted that the similarity of the fetal toxicokinetic profile for several models highly depends
262 on the assumption that only first order processes are involved in the placental transfer. If
263 saturation in one of the diffusion processes was modelled and occurred at the testing dose, the
264 fetal profiles will surely present dissimilarities.

265 We found four equations describing the J class model structure, *i.e.* the distribution between
266 the fetus and the mother is governed by a simple diffusion. They are presented in Supplementary
267 Material as J1 to J4 classes equations. The class J1 model consider the transfer between the
268 fetal tissue and the placental tissue, as shown in Gentry et al. [53]. Whereas the J2 to J4 classes
269 equations consider that the transfer occurred from the fetal blood and so present a fetal tissue
270 to blood partition coefficient. Some other models assigned to class J do not present placental
271 transfer equations in their publications and do not use a fetal tissue to blood partition coefficient
272 [46, 54, 55], so we supposed that they use the J1 class equation for placental transfer. Figure
273 7B presents the fetal tissue kinetic profiles for group 2 models (classes I, J1, J2, J3, J4 and L)
274 and the fetal blood pharmacokinetic profile for class K model. The steady-state fetal
275 concentrations of class J sub-models reach different values. Simulated fetal steady-state
276 concentrations with the J4 class model was more than seven-fold higher than those obtained

with the J1 class model. Those differences came from the ways of including the placental tissue to blood and the fetal tissue to blood partition coefficients in placental transfer equations. It is also interesting to notice, that the simulated fetal concentration profiles with J2 and J3 class models reproduce the fetal profiles simulated (fetal PBPK compartment) by the A, D, E and G classes from group 1. Also, the simulated fetal concentration profile from the I class model reproduces the profile obtained with H class model. Again, we identified four subgroups of transfer according to the time taken to reach steady-state. Results are given as Supplemental Material (Table S2).

For each class, we also simulated the maternal internal dose (results not shown). The different categories of time to reach a new steady-state between model classes were equivalent to those observed with fetal concentration profiles. Nonetheless, the impact of the placental transfer on maternal concentration, defined as the variation in steady-state concentration in the Maternal PBPK compartment, was equal to 5% or less, except for L class models which reaches 10%.

3.2 PHYSIOLOGICAL PARAMETERS

In the following, we present the volumes and blood flows parameterization of placental compartments. In animal models, direct measurements of organ weight provide the placental volumes and in humans, several reviews are available for placental volumes parameterization [9, 10, 56].

Rodent pPBPK models mainly use the equations from O'Flaherty [57] to parameterize the dam blood flow to placenta according to embryological age [46, 50, 55, 58-65]. The O'Flaherty gestation model was based primarily on Buelke-Sam data [66, 67] which described the changes in tissue volumes and blood flow rates in rats during pregnancy. The increase in blood flow to the placenta (a mix between yolk sac and chorioallantoic placenta) is given by:

$$F_{pla} = N \times (0.02 \times F_{dec} + F_{cap}) \quad \text{(E5)}$$

where N is the number of concepti, F_{dec} the increase in cardiac output per conceptus (in L/day) during the period of the yolk sac prominence and F_{cap} the increase in blood flow (L/day) to the chorioallantoic placenta of the rat after day 12 of gestation. F_{dec} and F_{cap} are both dependent of the embryological age, expressed in days. In humans, several models parameterize placental blood flow according to a uterine blood flow (L/h) regression equation, fraction of gestational age (GA in weeks), reported by Abduljalil [9, 68-70].

$$Uterine\ blood\ flow = 1.71 + 0.2068 \times GA + 0.0841 \times GA^2 - 0.0015 \times GA^3 \quad \text{(E6)}$$

Others use the equation for placental blood flow (F_{pla} in L/h) proposed by Gentry [53] which depend on placental volume (V_{pla} expressed in L) [51, 71-73].

$$F_{pla} = 58.5 \times V_{pla} \quad \text{(E7)}$$

Some authors compute the plasma flow to placenta as one third of the fetal cardiac output [74, 75] based on ultrasound measurements [76]. In Valcke's paper [77], the placental blood flow represents 12% of the maternal cardiac output. Luecke [78] and Gaohua [45] proposed an allometric relation function of the total weight and a polynomial formula which depend on gestational age, respectively.

The fetal blood flow to the placenta in animal models [79, 80], when included, was parameterized from sheep data [81, 82] or was derived from the best fit of the model to the experimental data [83]. In humans, the fetal blood flow to the placenta was parameterized with ultrasound umbilical cord blood flow data [76, 84, 85].

3.3 PARTITIONING OF SUBSTANCES INTO THE PLACENTA

For all species, the partition coefficient between placental tissues and maternal blood (or plasma, as in the following) is parameterized from different sources depending on data

availability. In the absence of data, some authors set it equal to the partition coefficient of another compartment considered to have similar composition as the placenta (*e.g.,* the partition coefficient between rapidly perfused tissues and blood [40, 72, 86] or the liver over blood partition coefficient [87]). Others use an "arbitrary" value [88]. For animal models, it can also be directly estimated with *in vivo* data [55, 61, 63, 83]. In absence of equivalent human parameter value, it has also been set to a value estimated for animals in a human model [47]. Several authors used *in silico* predicted values from physicochemical properties and tissue composition data [89] or *ex vivo* data [70].

A placenta-to-fetal blood (or plasma, as in the following) partition coefficient is defined when the placental tissues and the fetal blood are integrated present in the model. Two cases can be considered: the placental tissues are assumed homogeneous or not. In the first case, the placenta-to-fetal blood partition coefficient can be assumed similar to the placenta-to-maternal blood partition coefficient. This approach is shared by the majority of the models. And most of the time, only one parameter is defined for partition between the placental tissue and blood [39, 55, 69-76, 99]. The placenta-to-fetal blood partition is different from the placenta-to-maternal blood if the model assumes that the maternal and fetal blood compositions differ [10, 90]. For instance, this approach was used for methyl-mercury [91]. Furthermore, in Kim's model [83], the placenta-to-fetal blood partition coefficient is computed with a maternal blood to fetal blood partition coefficient. When placental tissues are assumed heterogeneous, different tissue to blood partition coefficients can be used for the placental sub-compartments. In the model described in Dallmann et al. [89], the maternal placental interstitial tissue subcompartment to maternal plasma partition coefficient (Figure S1) and the fetal placental interstitial tissue subcompartment to fetal plasma partition coefficient are both computed as proposed by Schmitt [92]:

$$PC_{int,pls} = \left(f_{water}^{int} + \frac{f_{protein}^{int}}{f_{protein}^{pls}} \times \left(\frac{1}{fu} - f_{water}^{pls} \right) \right) \times fu \quad \text{(E8)}$$

with *fu*, f_{water}^{int}, $f_{protein}^{int}$, f_{water}^{pls} and $f_{protein}^{pls}$ the plasma free fraction of a substance, the fraction in water of the interstitial tissue, the fraction in protein of the interstitial tissue, the fraction in water of the plasma considered and the fraction in protein of the plasma considered, respectively. Volume fractions in water, protein, lipids, phospholipids *etc.* are given for the whole placenta and other organs related to pregnancy [10]. The model accounts for the changes of maternal albumin serum concentration, maternal α-1-glycoprotein acid serum concentration and *fu* according to fertilization age. The fetal placental intracellular tissue subcompartment to maternal plasma partition coefficient (Figure S1) was computed using QSAR models based on the physicochemical properties of the substance [92-94].

4 METHODS TO QUATITATIVELY ESTIMATE THE PLACENTAL TRANSFERS

In this section, we present methods that inform chemical transfer rates through the placenta. Those are *in silico* models, *in vitro* cell systems, *ex vivo* placental perfusion systems, animal and human data. They are discussed from the perspective of their contribution to the development or evaluation of pPBPK models.

4.1 IN SILICO MODELS

Several types of *in silico* models have been used in the literature. A semi-empirical equation that calculates the apparent permeability constant expressed in $[v].[t]^{-1}$ has been proposed by Dallmann et al. [61]. This is based on 2 parameters: the logarithm of the membrane affinity and the efficient molecular weight (*i.e.,* considering the presence of halogen atoms in the molecule). Although this approach is easy-to-use and interesting in a high-throughput perspective, the semi-empirical equation rationale is not given.

371 Quantitative Structure-Property Relationships (QSPRs) are statistical models which link a
372 biological property to physico-chemical descriptors of a substance. Several QSPRs have been
373 developed to predict the transfer of drugs and/or chemicals through the placental barrier in the
374 form of a transfer index or a concentration ratio of fetal to maternal (F:M) blood [95-100].
375 Giaginis et al. [95] collected clearance index (CI) values for 88 compounds from *ex vivo*
376 placental perfusion experiments with drugs belonging to different therapeutic classes
377 (analgesic, neuroleptic, antiviral *etc*.). From this dataset, Zhang et al. [98] developed a QSPR
378 defined by 48 molecular descriptors. The model was deemed to be robust with a good predictive
379 potential (r^2 = 0.9, q^2 = 0.7). Takaku et al. published a QSPR based on 3 descriptors using *in*
380 *vivo* human F:M ratio data [100].

381 Both QSPRs found a negative correlation between the molecular weight and chemical
382 placental transfer. Otherwise, conclusions on the relation between the polarity descriptors
383 (Topological polar surface area, TopoPSA, and maximum E-state of hydrogen atom, Hmax)
384 and placental transfer were dissimilar between the two QSPRs. In Takaku's paper, TopoPSA
385 and Hmax were positively correlated to chemical placental transfer while Zhang's QSPR
386 described a negative contribution. Takaku et al. assumed that the impact on the interaction of
387 compounds with blood lipids is ignored when *ex vivo* data are used in QSPR development,
388 because those experiments use a buffer as a proxy for maternal and fetal bloods. The latter failed
389 to reproduce the difference of lipid blood content between maternal and fetal blood *in vivo*. This
390 would promote the transfer of low polarity compounds because of the high lipid content in the
391 membrane, leading to the negative values of the polarity descriptors [100]. They also assume
392 that the positive values found for polarity descriptors in their QSPR might be attributed to the
393 influence of transporters on hydrophilic substances transfer.

394 The QSPRs currently available show the same limitations as their data sources, i.e. they are
395 adequate to predict the placental transfer rates at the end of the pregnancy. Their predictions

396 could be interpreted together with a pPBPK model to account for the maternal and fetal
397 toxicokinetics and extrapolate to other gestation periods. For instance, the QSPR estimates
398 could be used as a basis for fitting placental transfer parameter. However, no such methods
399 were found in the literature.

400 ***4.2 IN VITRO MODELS***

401 Choriocarcinoma cells (BeWo, Jeg-3 and JAR cells) can be used to study transcellular
402 transport between an apical (maternal-like) and a basolateral (fetal-like) compartments which
403 mimic the bi-compartmental structure of the placenta. They form tight-junctioned monolayer
404 when cultured on semi-permeable membrane and display many of the biochemical and
405 morphological characteristics reported for *in utero* invasive trophoblast cells [101] but some
406 functions should be altered since they derived from placenta choriocarcinoma. For instance, the
407 active transport should be decreased since the levels of multidrug resistance (MDR) 1/P
408 glycoprotein (Pgp) mRNA and protein expression were reduced in BeWo and JAR cells
409 compared to trophoblast primary cells [102]. The BeWo cell line is particularly attractive
410 because it is stable and grows to a confluent monolayer in a relatively short period of time [103].
411 Apparent permeability (P_{app} usually in cm/s) for the *in vitro* system can be estimated:

412 $$P_{app} = \frac{Q}{A \times t \times C_d} \quad \text{(E9)}$$

413 where Q is the amount of substance in the receiver chamber at time t, A is the diffusion surface
414 area and C_d is the concentration of substance in donor chamber. It should be corrected for the
415 influence collagen-coated polycarbonate membranes to yield the apparent permeability
416 coefficient (P_e) of the BeWo monolayer.

417 $$\frac{1}{P_{app}} = \frac{1}{P_c} + \frac{1}{P_e} \quad \text{(E10)}$$

where P_c is the apparent permeability coefficient of the collagen-coated polycarbonate membrane alone.

For a test set of 11 compounds, the relative P_{app} to antipyrine in the *in vitro* BeWo model were in good correlation with the transfer indices from *ex vivo* studies reported in the literature [104]. Parallelly, Poulsen et al. [105] show for caffeine, benzoic acid glyphosate and antipyrine that although both the *in vitro* and *ex vivo* models classify the steady-state percentage of substance transported in a similar rank order, the time to equilibration observed for the *in vitro* system is ten time longer than for the placental perfusion experiments. Unlike in placental perfusion model, the choriocarcinoma system do not capture the multilayered structure of chorionic villi and do not integrate placental blood flows, rendering difficult the extrapolation to *in vivo* situations.

Several recent works proposed new *in vitro* systems which may be closest to *in vivo* conditions. To account for barrier function of endothelial cells, Aengenheister et al. developed a co-culture approach of BeWo b30 cells, a clone of BeWo cells, and placental microvascular endothelial cells (HPEC-A2) under static and shaken conditions [106]. The co-culture transfer model was tested with four substances and two polystyrene nanoparticles [106]. The authors measured fetal-like basolateral amount change over 24 hours. For antipyrine and indomethacin, they concluded that translocation profiles across either BeWo and HPEC-A2 monolayers or the co-culture were similar. Previously, Lee et al. [107] and Blundell et al. [108] developed bilayers *in vitro* microfluidic systems, properly called placenta on-a-chip systems. To reproduce the trophoblasts layer Lee et al. used Jeg-3 cells and Blundell et al. used BeWo cells. For the endothelial layer, Lee et al. used human umbilical vein endothelial cells (HUVECs) and Blundell et al. used human primary placental villous endothelial cells (HPVECs). Both publications present the percent rate of glucose transfer from the maternal-like to the fetal-like compartments supposedly at the final time. The rate of glucose transfer was calculated as the

443 percentage of venous fetal concentration of a substance with respect to the maternal
444 concentration. Lee et al. also computed a glucose permeability coefficients (GP) and a glucose
445 permeability coefficient of an unsupported cell monolayer (GP_{UM}) which respectively
446 correspond to the definition of a P_{app} and a P_e. Another recent article assesses the adverse impact
447 of nanoparticles on placental barrier with a placenta on-a-chip microdevice system [109]. The
448 placental barrier integrity was partly captured by microscopy measures of the transfer of FITC-
449 dextran (MW 10000 Da) across the placental barrier. Finally, further improvements have been
450 made in glucose [110] and cholesterol [111] transfer studies using primary trophoblast cells
451 isolated from healthy placentas delivered at term, attempting to bypass choriocarcinoma cells
452 limitations. They might later be applied to study the diffusion of xenobiotics, as well as
453 intracellular metabolism, paracellular contributions and carrier-mediated mechanisms
454 influencing the vectorial transport of molecules.

455 Several works demonstrated that such *in vitro* data are valuable for the development of
456 pPBPK models [34, 87, 112]. For a series of phenolic compounds, Strikwold et al. extrapolated
457 the apparent placental diffusional constants from P_{app} values estimated with a BeWo b30 cell-
458 based system and used them into a rat pPBPK model [87]. To estimate the placental diffusion
459 of a substance, the P_{app} value was scaled to an *in vivo* transplacental diffusion clearance rate
460 with the measured P_{app} value of antipyrine and the *in vivo* measured antipyrine clearance rate
461 [113] scaled to the 11^{th} gestational day. Zhang et al. developed a similar approach with
462 midazolam as the reference compound [34, 112]. The unbound transplacental passive diffusion
463 clearance of two therapeutic compounds (zidovudine and theophylline) were computed using
464 their *in vitro* apparent permeability P_{app} values and the *in vivo* diffusion clearance of midazolam
465 estimated from umbilical vein plasma concentrations [114].

4.3 EX VIVO PLACENTAL PERFUSION SYSTEMS

The first placental *ex vivo* system was published by Panigel et al. [115] and was then improved [116, 117] notably with the isolated perfused cotyledon model. The latter consists in the perfusion of a placental lobule, which contains a cotyledon, at the interface of a maternal-like and a fetal-like chambers. *Ex vivo* methods restitute structurally the anatomy of the site of transfer and temporally mimics experimentally the physiological conditions of a human placenta in the third trimester of pregnancy or at term [101]. The collection of absolute chemical content in the three compartments (maternal-like, placental, fetal-like) over time allows to estimate the transfer rates of substances through the placenta. The maternal/fetal circulation systems can be "open/open" (*i.e.,* the single pass model), "open/closed", "closed/open" or "closed/closed" (*i.e.,* the dual recirculating model), with "open" qualifying a non-recirculating perfusate and "closed" a recirculating one. The dual recirculating model is close to physiologic conditions and allows studying chemical distribution (percentage of transfer) in the system and exploring involved mechanisms, whereas an open circuit is used sequentially to compute clearances under steady-state condition in maternal-like chamber [118]. The transfer rate estimated for a chemical is often normalized by antipyrine transfer measures to account for inter-placental and experimental variability (difference in the flow rates, the use of perfusion medium, the use of plasmatic proteins or the surface area of exchange *etc.*). This reference compound is an intermediate lipophilic substance which does not bind to plasma and tissue proteins, is not metabolized in the placenta and diffuses passively through lipid membranes [118]. Hutson et al. evaluated the *ex vivo* system predictions for F:M concentration ratios at steady-state against *in vivo* umbilical cord-to-maternal blood (C:M) concentration ratios and observed a significant correlation [119] (F:M ratios were adjusted for the differences in protein binding and pH between fetal and maternal bloods and outliers were excluded, $r^2 = 0.85$, $p < 0.001$).

The computation of the transfer rates from the *ex vivo* experiments differ between authors. It can be expressed as a transfer rate constant or a clearance [118]. Most of the time, the results are given as a ratio of the selected output with the corresponding output for antipyrine. The ratios are either transfer indexes (TIs) [120] or clearance indexes (CIs) [121]. Ala-Kokko et al. [118] define the latter as the rate of extraction of a compound from the maternal circulation towards the fetal circulation, and integrate the fetal perfusion rate parameter in its computation. Other publications [122-124] computed, for a specific period of time (generally up to 90 min), the fetal transfer rate (FTR, ratio of venous fetal concentration of a substance over maternal concentration) and a clearance index (CLI) as the ratio of the FTR of a substance over the FTR of antipyrine (the fetal perfusion rate is not included in CLI computation).

The placenta can act as a reservoir for some lipophilic compounds. The *ex vivo* system offer to estimate placental tissue binding. For instance, tacrolimus (an immunosuppressive drug) was observed to strongly accumulate in placental tissues but did not reach the fetal-like compartment [125]. In addition to placental and fetal chemicals exposure assessment, the *ex vivo* placental perfusion model allows to study the effect of endogenous (albumin, biogenic amines etc.) or exogenous substances on placental transfer and fetal perfusion [101].

Although they are static measurements, FTRs, CLIs, CIs and TIs could be used in pPBPK modeling as steady-state values for placental diffusional transfer parameter estimation. However, those *ex vivo* system outputs summary information and more dynamic data are of greater interest for toxicokinetic model development. Some authors scaled *in vivo* placental diffusion rate with *ex vivo* experimental raw data for pPBPK model parameterization [70, 126, 127]. In this attempt, researchers firstly compute a rate accounting for a single cotyledon with *ex vivo* fetal and maternal reservoirs concentration-time data [70, 127]. Although they share a similar approach, De Sousa Mendes et al. estimate this diffusion rate with a non-linear mixed effect model [70] whereas Schalwijk et al. used the slope of the natural log concentration time

profile of the perfusion reservoir [127]. Schalwijk et al. estimate asymmetric values of exchange between the maternal-like and fetal-like reservoirs. Secondly, the estimated diffusion parameter for a single isolated cotyledon were scaled to the whole placenta. De Sousa Mendes et al. used the volume ratio between the placenta and the cotyledon, and Schalwijk et al. the average number of cotyledons per placenta.

4.4 ANIMAL MODELS

Animal-based experimental methods are the main information supplier of placental diffusional transfer rates in pPBPK modeling studies (Tables 1 and 2), mainly as they are easy to operate with low inter-individual variation because of inbred animals, they offer to study placental transfer at different gestation ages and are whole body system which integrate the physiological changes due to pregnancy. *In vivo* animal data were used both in animal [50, 58, 79, 86, 128, 129] and human [73, 130] pPBPK models and most of the time for environmental chemicals. The experiments were conducted in different animal species (rats, mice, guinea pig, rabbits, sheep, pig, non-human primates *etc.*). *In vivo* studies consist in sampling biological matrices (blood, urine, feces, placenta *etc.*) in the mother and the fetus(es) at different times after the administration of a defined dose of chemical by a specific maternal route. The multiple maternal and fetal concentration time profiles permit to estimate mother-to-fetal and fetal-to-mother diffusional transfer constants. Moreover, it is noteworthy that animal studies allow to examine chemical accumulation in placental and fetal tissues.

However, *in vivo* animal models present some limitations for translation to human due to differences in placental macrostructure, maternofetal tissue layers type and hemodynamics. The human placental villous internal structure and multi-villous blood flow pattern is shared with macaques while mice, rats, rabbits and guinea pig show labyrinthic placental structures and countercurrent blood flows [131]. In humans, the structure of tissue layers which separate maternal and fetal bloods, defined by Grosser classification [132], is haemomonochorial.

Among laboratory animals, guinea pig, chinchilla and rhesus monkey present haemomonochorial placental barrier and are then relevant for animal-to-human extrapolation. Furthermore, the number of fetuses per litter and duration of gestation are close to human values [133]. However, the placental active transport capacity of an animal model will depend on the level of expression of specific transport proteins located in the trophoblast and fetal endothelial cells. Since transporters are substrate-specific, the assessment of the active transport of hydrophilic compounds will probably necessitate high specificity in animal models or the use of genetically modified animals.

4.5 HUMAN DATA

Although drug and chemical exposure studies in pregnant women are limited, maternal blood and tissues sampling during gestation, and cord blood sampling near the time of delivery are valuable sources of information in perinatal exposure assessment [118]. In drug monitoring studies (most of the time for drugs with narrow therapeutic windows or used in fetal therapy), numerous single blood samples from different pregnant women are joined (a same pregnant women could also be sampled at different occasions). When they are available, single cord samples are paired to maternal samples at delivery. Time between administration and collection are recorded allowing to draw maternal and fetal blood concentration-time profiles, informing about transplacental transfer for a short time period. Those data are often used in population pharmacokinetic studies attempting to explain between-subject variabilities with various pertinent covariates [134]. Multiple samples can also be collected in only one mother to establish an individual maternal time-course profile [12]. For environmental pollutants, general population biomonitoring studies give a picture of concentration levels in biological matrices for many compounds in a specific population. Maternal blood or urine can be sampled across all gestation period, at delivery and postpartum [135, 136]. Direct parent compound measures are not always feasible, notably for rapid metabolized compounds, and sampling the metabolites

as biomarkers is common. Some studies provide concentration data in other types of fetal or neonates matrices like teeth [137], meconium [138] or amniotic fluid [139].

Cord blood sampling at term serves as a proxy for fetal blood. It allows computing a F:M blood concentrations ratio which reflects the degree of chemical transfer from the mother to the fetus at birth [140]. The F:M ratio should be interpreted with caution. For substances with short biological half-life, this output is highly variable, even on a time scale of a few hours. The partitioning between cord and maternal blood will depend on the time spent between sampling and the last exposure. Therefore, frequency and duration of mother's exposure, relative timing of sampling of maternal and cord bloods, and the time of delivery are needed to correctly interpret a F:M ratio [27]. Ideally, if population toxicokinetic measures are available, a ratio based on the area under the curve (AUC) would be more desirable since it is more representative of exposures. Also, the concentration-based F:M ratio does not provide any information about distribution of a substance within the fetal tissues. In this perspective, Cao et al. measured bisphenol A in placental tissue and liver samples from aborted fetuses (fetal age from 10 to 20 weeks) from 1998 to 2008 [141]. In 2014, Aylward et al. published a review on available maternal and cord blood concentration data in literature [6]. It provides data from more than 100 studies on F:M concentration ratios for persistent environmental pollutants (organochlorine pesticides, polychlorinated biphenyls, perfluorinated compounds *etc*.). On that basis, chemical classes with a high degree of placental transfer were identified. The reported ratios of central tendency measures were generally between 0.1 and 1 indicating that cord blood concentrations were lower or equal to maternal concentrations. For some compounds, like brominated flame-retardant compounds, polyaromatic hydrocarbons or metals, the reported ratios of central tendency measures were above 1. Reported data did not always came from maternal/infant pairs and ratios were computed either on a wet weight basis or with lipid adjusted measurements. Note that lipid concentrations are three-time higher on average in maternal serum than in cord

591 serum [142]. The review highlighted the high degree of point estimates variations for a given
592 chemical across studies (an order of magnitude or more), with an inability to discern uncertainty
593 from true variability.

594 Maternal and fetal sampling data have been used to inform placental transfer rates in pPBPK
595 models, mostly for environmental chemicals (Table 1 and Table 2). For instance, after
596 transposing transfer parameters from a previous rat model for PFOS and PFOA [63] to a life-
597 stages PBPK model in human [51], Loccisano et al. re-calibrated those parameters to yield the
598 human maternal:fetal concentration ratios observed at delivery in biomonitoring studies.
599 Authors also frequently used maternal concentration-time data to evaluate the pPBPK model
600 simulations [89, 112]. De Sousa et al. evaluated the capacity of their pPBPK model to predict
601 maternal and fetal concentration profiles after nevirapine intake in late pregnancy with drug
602 monitoring observations for mothers and fetuses [70].

603 **5 DISCUSSION**

604 The Developmental Origins of Health and Disease (DOHaD) theory hypothesizes that the
605 fetal environment during critical periods of development and growth may influences
606 individual's short- and long-term health [143]. However, human fetal internal chemical
607 exposure is difficult to assess throughout gestation due to ethical reasons. *In silico* tools as
608 pPBPK models can simulate the fetal internal exposures in several organs at different times of
609 the pregnancy as an alternative. These models rely on indirect or incomplete data, *e.g., in vitro*,
610 *ex vivo*, animal to inform their placental transfers parameters. Those exposures depend on
611 maternal and fetal ADME processes but also mainly on placental transfers of chemicals.

612 In pPBPK modeling publications, the choice of the placental transfer structure is rarely
613 discussed. However, we demonstrated, using model simulations with the various placental
614 transfer framework identified in the scientific literature, that the structure impacts fetal

615 toxicokinetics, *e.g.*, the time to reach steady-state after a substance single dose in a closed model
616 (No elimination was included in maternal or fetal sub-models to focus on the placental transfer
617 process). Our model simulations showed that different structures can lead to similar maternal
618 and fetal profiles. In addition to matching the prediction objectives of a particular study, the
619 choice of the model structure should consider the number of parameters to inform and the
620 complexity of the model. For instance, we recommend using J2 or J3 class equations for
621 placental transfer if no fetal sub-model is included. In our simulation scenario, they reproduced
622 the simulated profiles obtained with A, D, E and G classes equations in both the time to reach
623 steady-state and the fetal internal concentration.

624 Further efforts to account for placental structural properties which impact passive diffusion
625 should be integrated in pPBPK models. Although the maternal blood perfusion from spiral
626 arteries is efficient only around the 12th week of GA, this modification in the placental transfers
627 between the first and second trimesters is rarely described in pPBPK models. A two-sequence
628 structure would better describe the early and late transfers to the fetus and the resulting fetal
629 exposure. These two phases are present in the new "P" class structure we propose. The early
630 phase structure consists in three placental compartments: maternal flow-limited placental tissue,
631 diffusion-limited intervillous space, and fetal flow-limited placental tissue (Figure 8). The latter
632 switches to an E class structure when the time of the intervillous space perfusion by spiral
633 arteries is reached. The structural reorganization (lumping of the maternal placental tissue and
634 intervillous space) can be simply simulated by a parametric change, setting the diffusion
635 between maternal placental tissue and intervillous space to a very high arbitrary value. Given
636 the uncertainty upon the maturation of the utero-placental circulation in the first trimester
637 (lacunae, trophoblastic plugs etc.), we assumed that the diffusional constant between the
638 maternal placental tissue and the intervillous space compartment stands for the limitation of
639 transfer during this period and was defined as a percentage of the maternal blood flow. The

choice of a diffusion process is supported by the assumption that the trophoblast cells meet some maternal blood during their incursion within the endometrial mucosa based on several articles [17, 26, 144]. However quantitative data are lacking for a proper parametrization of this process. We simulated fetal internal concentration, with the same single dose exposure scenario used previously, with the early and late phases P class placental transfer structures (parameterization is shown in Table S4). As expected, the model reproduces the B and C classes' profiles with the early phase structure (Figure 7), and as the A, D, E and G classes' profiles with the late phase structure (not shown).

In almost every pPBPK model reviewed, passive diffusion is included. However, active transport and metabolism in the placenta are often neglected, contributing to much uncertainty in fetal exposure assessment of potential substrates [29, 145]. We identified six pPBPK models which included an active mechanism of placental uptake/efflux (Table 3) in addition to diffusion. The majority were developed for perchlorate and iodide kinetics in rats and humans [40, 47, 65, 80]. These models included a unidirectional uptake from the mother to the fetus which was described with Michaelis-Menten parameters (K_m and V_{max}). The K_m were taken from thyroid slices data [146, 147], and the V_{max} were estimated during model calibration. Among the 50 reviewed publications, five [34, 73, 78, 126, 148] included an elimination parameter from the placental compartment which can be considered as a placental metabolism. For instance, Sharma et al. integrated the glucuronidation of bisphenol A in the placental compartment in their pPBPK model [71]. They extrapolated to *in vivo* K_m and V_{max} parameter values obtained from a hepatic cell-line with data on bodyweight, placental volume and microsomal content. Furthermore, Shintaku et al. and De Sousa Mendes et al. estimated a first-order elimination constant by fitting placental *ex vivo* data to account for placental metabolism [126, 148]. In a recent paper, Zhang et al. have shown through simulations that placental metabolic or placental transport clearances can significantly determine fetal drug exposure if

665 the magnitude of these clearances is comparable to that of passive diffusion (likely for
666 hydrophilic substances) [34]. Because we focus on the transplacental transfer in pPBPK models,
667 this review did not address certain aspects influencing the fetal internal exposure such as the
668 fetal metabolism. Although the latter is rarely included in pPBPK models, the presence of
669 metabolic enzymes has been reported in fetal hepatocytes [149, 150]. Furthermore, levels of
670 fetal hepatic cytochrome P450 enzymes vary with fetal development [151]. Levels of transport
671 proteins and metabolic enzymes in the placenta also change during pregnancy and could impact
672 the transplacental transfer of chemicals [152]. For instance, the expression of ABCB1 proteins
673 in the apical membrane of syncytiotrophoblast decreases throughout pregnancy [14]. Despite
674 this, little is quantitively known about their ontogeny in placental cells [153]. Some researchers
675 have attempted to do an "expression cartography" of trophoblast drug transporters genes in
676 early and late gestation based on ARNm expression in trophoblast primary cells [154].

677 Some other aspects of the available models could be improved in future developments.
678 Although membrane thickness is a parameter of Fick's law, the thinning of the trophoblast layer
679 is not accounted for in pPBPK models published so far. Its integration will probably not impact
680 much the maternal kinetic profile of a substance. However, the time to reach steady-state in
681 fetal compartments, after a maternal exposure in the late pregnancy, might be reduced since the
682 diffusion transfer rate is higher. The placenta-to-fetal blood partition coefficient value was set
683 equal to the placenta-to-maternal blood partition coefficient in almost every reviewed models
684 despite the fact that lipid concentration in maternal blood is different from fetal lipid
685 concentration [142]. However, the placenta-to-fetal blood partition coefficient should be a
686 highly sensitive parameter for fetal concentration. When possible, we recommend using a
687 specific value for this critical parameter. When maternal and fetal placental tissues are assumed
688 homogenous, modelers could use a fetal to maternal blood partition coefficient, as proposed by

689 Kim et al. [83]; and when placental tissues are assumed heterogeneous, partition coefficients
690 could be computed with an algorithm that consider their compositions.

691 The main difficulty in diffusion-limited placental transfer modeling might be the estimation
692 of the diffusion rate throughout all gestation. It is generally inferred from animal *in vivo* kinetic
693 studies, but not always scaled to the target species. Also, expensive and time-consuming
694 animal-based methods are not suitable for high-throughput safety assessment [155], while
695 ethical and economic reasons are motivating a reduction in the number of animal studies.
696 Human data are often only one point at term per subject with large interindividual variations.
697 Despite strong assets, the *ex vivo* methodology presents some limits: a low experimental success
698 rate, the need of fresh placentas and it cannot be used to determine transfer in the first trimester.
699 It does not seem appropriate for high throughput either [106]. *In vitro* methods can meet this
700 challenge but are criticized for their lack of effective representation of complex *in vivo* systems.
701 *In silico* tools are promising in high throughput perspective, but as mentioned previously, the
702 QSPRs show the same limitations as their data sources. Although of interest, in our opinion,
703 there is no QSPR model to predict apparent permeabilities from trophoblastic cells data. Such
704 a model would provide high-throughput estimates of placental transfer for pPBPK models.

705 Fetal exposure to xenobiotics during the first trimester is thought to be critical for
706 development. Unfortunately, most of the pPBPK models are based on the placental structure at
707 the end of pregnancy, preventing to correctly estimate fetal risks. Here, the P model provides a
708 new mechanistic based approach to better characterize the relationship between the exposure
709 dose and the adverse effects by modeling the fetal internal exposure during this window of
710 sensitivity. Based on physiological observations, the model can simulate the fetal internal
711 exposure of a xenobiotic during the whole gestation period, including the first trimester. This
712 model could be implemented in a generic pPBPK model and used in risk assessment to better
713 characterize the fetal exposures. For instance, the model can help in estimating the fetal internal

chemical exposure threshold values associated with maternal biomonitoring equivalents at each trimester for a series of compound, or it can predict the fetal internal levels of cumulative pollutants based on maternal or cord blood biomonitoring data. Furthermore, this model can also be suitable in an exposome approach by integrating the gestation exposure dynamics in epidemiological studies analysis to provide better understanding of the link between prenatal exposure and health effects.

In conclusion, our review highlights the various practices to account for chemical placental transfers in pPBPK modeling. They are eight transfer structures when a fetal sub-model is included (group 1) and four if not (group 2). Two structure classes are more used than others, D class and J class structures for group 1 and group 2 models, respectively. That must be qualified by the fact that the recent publications tend to the development of much more complex structures (*e.g.,* A and B classes) for group 1 models, while the J class model presents different sub-classes. It seems that there is no clear consensus in the field. We also underline the fact that information available for placental transfer parameterization (partition coefficients, blood flows, diffusion constants *etc.*) and their justification were inequal across the reviewed articles. Placental transfer in pPBPK modeling is promised to further development to improve fetal pharmacokinetic modeling. This will require the development of new quantitative data to evaluate the models, and enzyme expression data to describe metabolism and active transport in the placenta. The availability of such data for different phases of gestation would certainly improve the quality of developmental toxicity assessment.

6 AKNOWLEDGEMENTS

We thank Clémentine Garoche for drawing Figure 1.

7 FUNDING

This work has received funding from the European Union's Horizon 2020 Research and Innovation programme under Grant Agreement No 825712 (OBERON project).

8 REFERENCES

1. Saoudi, A., et al., *Prenatal exposure to lead in France: Cord-blood levels and associated factors: Results from the perinatal component of the French Longitudinal Study since Childhood (Elfe).* International Journal of Hygiene and Environmental Health, 2018. **221**(3): p. 441-450.
2. Philippat, C., et al., *Exposure to Phthalates and Phenols during Pregnancy and Offspring Size at Birth.* Environmental Health Perspectives, 2012. **120**(3): p. 464-470.
3. Howard, S.G., *Developmental Exposure to Endocrine Disrupting Chemicals and Type 1 Diabetes Mellitus.* Frontiers in endocrinology, 2018. **9**: p. 513-513.
4. Heindel, J.J., et al., *Developmental Origins of Health and Disease: Integrating Environmental Influences.* Endocrinology, 2015. **156**(10): p. 3416-3421.
5. Sturza, J., et al., *Prenatal exposure to multiple pesticides is associated with auditory brainstem response at 9months in a cohort study of Chinese infants.* Environment International, 2016. **92-93**: p. 478-485.
6. Aylward, L.L., et al., *Relationships of chemical concentrations in maternal and cord blood: a review of available data.* Journal of Toxicology and Environmental Health, 2014. **Part B**(17): p. 175–203.
7. Andrew, M.A., M.F. Hebert, and P. Vicini. *Physiologically based pharmacokinetic model of midazolam disposition during pregnancy*. in *30th Annual International Conference of the IEEE Engineering in Medicine and Biology Society*. 2008.
8. Beaudouin, R., S. Micallef, and C. Brochot, *A stochastic whole-body physiologically based pharmacokinetic model to assess the impact of inter-individual variability on tissue dosimetry over the human lifespan.* Regulatory Toxicology and Pharmacology, 2010. **57**(1): p. 103-116.
9. Abduljalil, K., et al., *Anatomical, Physiological and Metabolic Changes with Gestational Age during Normal Pregnancy.* Clinical Pharmacokinetics, 2012. **51**(6): p. 365-396.
10. Dallmann, A., et al., *Gestation-Specific Changes in the Anatomy and Physiology of Healthy Pregnant Women: An Extended Repository of Model Parameters for Physiologically Based Pharmacokinetic Modeling in Pregnancy.* Clinical Pharmacokinetics, 2017. **56**(11): p. 1303-1330.
11. Ke, A.B., et al., *A physiologically based pharmacokinetic model to predict disposition of CYP2D6 and CYP1A2 metabolized drugs in pregnant women.* Drug metabolism and disposition: the biological fate of chemicals, 2013. **41**(4): p. 801-813.

12. Jogiraju, V.K., et al., *Application of physiologically based pharmacokinetic modeling to predict drug disposition in pregnant populations.* Biopharmaceutics & Drug Disposition, 2017. **38**(7): p. 426-438.

13. Corley, R.A., et al., *Evaluation of Physiologically Based Models of Pregnancy and Lactation for Their Application in Children's Health Risk Assessments.* Critical Reviews in Toxicology, 2003. **33**(2): p. 137-211.

14. Myllynen, P. and K. Vähäkangas, *Placental transfer and metabolism: An overview of the experimental models utilizing human placental tissue.* Toxicology in Vitro, 2013. **27**(1): p. 507-512.

15. Burton, G.J. and E. Jauniaux, *What is the placenta?* American Journal of Obstetrics & Gynecology, 2015. **213**(4): p. S6.e1-S6.e4.

16. Myren, M., et al., *The human placenta – An alternative for studying foetal exposure.* Toxicology in Vitro, 2007. **21**(7): p. 1332-1340.

17. Gude, N.M., et al., *Growth and function of the normal human placenta.* Thrombosis Research, 2004. **114**(5): p. 397-407.

18. Beghin, D., *Le passage placentaire des médicaments.* Revue de médecine périnatale, 2014. **6**(1): p. 12-20.

19. Rothbauer, M., et al., *A comparative study of five physiological key parameters between four different human trophoblast-derived cell lines.* Scientific Reports, 2017. **7**(1): p. 5892.

20. Fowden, A.L. and A.J. Forhead, *Endocrine Regulation of Feto-Placental Growth.* Hormone Research in Paediatrics, 2009. **72**(5): p. 257-265.

21. Giaginis, C., S. Theocharis, and A. Tsantili-Kakoulidou, *Current toxicological aspects on drug and chemical transport and metabolism across the human placental barrier.* Expert Opinion on Drug Metabolism & Toxicology, 2012. **8**(10): p. 1263-1275.

22. Griffiths, S.K. and J.P. Campbell, *Placental structure, function and drug transfer.* Continuing Education in Anaesthesia Critical Care & Pain, 2015. **15**(2): p. 84-89.

23. Huppertz, B., *The anatomy of the normal placenta.* Journal of Clinical Pathology, 2008. **61**(12): p. 1296.

24. Lewis, R.M., et al., *The Placental Exposome: Placental Determinants of Fetal Adiposity and Postnatal Body Composition.* Annals of Nutrition and Metabolism, 2013. **63**(3): p. 208-215.

25. Aherne, W. and M.S. Dunnill, *Morphometry of the human placent.* British Medical Bulletin, 1966. **22**(1): p. 5-8.

26. Burton, G.J., et al., *Uterine Glands Provide Histiotrophic Nutrition for the Human Fetus during the First Trimester of Pregnancy.* The Journal of Clinical Endocrinology & Metabolism, 2002. **87**(6): p. 2954-2959.

27. Sastry, B.V.R., *Techniques to study human placental transport.* Advanced Drug Delivery Reviews, 1999. **38**(1): p. 17-39.

28. Shu-Feng, Z., et al., *Placental Drug Disposition and Its Clinical Implications.* Current Drug Metabolism, 2008. **9**(2): p. 106-121.

29. Syme, M.R., J.W. Paxton, and J.A. Keelan, *Drug Transfer and Metabolism by the Human Placenta.* Clinical Pharmacokinetics, 2004. **43**(8): p. 487-514.

30. Prouillac, C. and S. Lecoeur, *The Role of the Placenta in Fetal Exposure to Xenobiotics: Importance of Membrane Transporters and Human Models for Transfer Studies.* Drug Metabolism and Disposition, 2010. **38**(10): p. 1623.

31. Gundacker, C., et al., *Genetics of the human placenta: implications for toxicokinetics.* Archives of Toxicology, 2016. **90**(11): p. 2563-2581.

32. Jovelet, C., et al., *Inhibiteurs de tyrosine kinase et grossesse : quels risques pour le fœtus ?* Bulletin du Cancer, 2016. **103**(5): p. 478-483.

33. Vizcaino, E., et al., *Transport of persistent organic pollutants across the human placenta.* Environment International, 2014. **65**: p. 107-115.

34. Zhang, Z., et al., *Development of a Novel Maternal-Fetal Physiologically Based Pharmacokinetic Model I: Insights into Factors that Determine Fetal Drug Exposure through Simulations and Sensitivity Analyses.* Drug Metabolism and Disposition, 2017. **45**(8): p. 920.

35. Heikkinen, E.M., et al., *Foetal Fentanyl Exposure and Ion Trapping after Intravenous and Transdermal Administration to the Ewe.* Basic & Clinical Pharmacology & Toxicology, 2016. **120**(2): p. 195-198.

36. Maruyama, W., et al., *Simulation of dioxin accumulation in human tissues and analysis of reproductive risk.* Chemosphere, 2003. **53**(4): p. 301-313.

37. Pilari, S., C. Preuße, and W. Huisinga, *Gestational influences on the pharmacokinetics of gestagenic drugs: A combined in silico, in vitro and in vivo analysis.* European Journal of Pharmaceutical Sciences, 2011. **42**(4): p. 318-331.

38. Clewell, H.J., et al., *A physiologically based pharmacokinetic model for retinoic acid and its metabolites.* Journal of the American Academy of Dermatology, 1997. **36**(3, Supplement): p. S77-S85.

39. Faustman, E.M., et al., *Biologically based dose-response models for developmental toxicants: lessons from methylmercury.* Inhalation Toxicology, 1999. **11**(6-7): p. 559-572.

40. Lumen, A., D.R. Mattie, and J.W. Fisher, *Evaluation of Perturbations in Serum Thyroid Hormones During Human Pregnancy Due to Dietary Iodide and Perchlorate Exposure Using a Biologically Based Dose-Response Model.* Toxicological Sciences, 2013. **133**(2): p. 320-341.

41. Gabrielsson, J.L. and L.K. Paalzow, *A physiological pharmacokinetic model for morphine disposition in the pregnant rat.* Journal of Pharmacokinetics and Biopharmaceutics, 1983. **11**(2): p. 147-163.

42. Gabrielsson, J.L., L.K. Paalzow, and L. Nordström, *A physiologically based pharmacokinetic model for theophylline disposition in the pregnant and nonpregnant rat.* Journal of Pharmacokinetics and Biopharmaceutics, 1984. **12**(2): p. 149-165.

43. Gabrielsson, J.L., et al., *Analysis of pethidine disposition in the pregnant rat by means of a physiological flow model.* Journal of Pharmacokinetics and Biopharmaceutics, 1986. **14**(4): p. 381-395.

44. Krishnan, K., *Physiologically Based Pharmacokinetic Models in the Risk Assessment of Developmental Neurotoxicants*, in *Handbook of Developmental Neurotoxicology*, W. Slikker, M.G. Paule, and C. Wang, Editors. 2018, Academic Press. p. 539-557.

45. Gaohua, L., et al., *A pregnancy physiologically based pharmacokinetic (p-PBPK) model for disposition of drugs metabolized by CYP1A2, CYP2D6 and CYP3A4.* British journal of clinical pharmacology, 2012. **74**(5): p. 873-885.

46. Crowell, S.R., et al., *Impact of pregnancy on the pharmacokinetics of dibenzo[def,p]chrysene in mice.* Toxicological sciences : an official journal of the Society of Toxicology, 2013. **135**(1): p. 48-62.

47. Clewell, R.A., et al., *Perchlorate and Radioiodide Kinetics Across Life Stages in the Human: Using PBPK Models to Predict Dosimetry and Thyroid Inhibition and Sensitive Subpopulations Based on Developmental Stage.* Journal of Toxicology and Environmental Health, Part A, 2007. **70**(5): p. 408-428.

48. Emond, C., L.S. Birnbaum, and M.J. DeVito, *Physiologically Based Pharmacokinetic Model for Developmental Exposures to TCDD in the Rat.* Toxicological Sciences, 2004. **80**(1): p. 115-133.

49. Martin, S.A., et al., *Use of novel inhalation kinetic studies to refine physiologically-based pharmacokinetic models for ethanol in non-pregnant and pregnant rats.* Inhalation Toxicology, 2014. **26**(10): p. 598-619.

50. Lin, Z., et al., *Estimation of placental and lactational transfer and tissue distribution of atrazine and its main metabolites in rodent dams, fetuses, and neonates with physiologically based pharmacokinetic modeling.* Toxicology and Applied Pharmacology, 2013. **273**(1): p. 140-158.

51. Loccisano, A.E., et al., *Development of PBPK models for PFOA and PFOS for human pregnancy and lactation life stages.* Journal of toxicology and environmental health. Part A, 2013. **76**(1): p. 25-57.

52. Bois, F.Y., *GNU MCSim: Bayesian statistical inference for SBML-coded systems biology models.* Bioinformatics, 2009. **25**(11): p. 1453-1454.

53. Gentry, P.R., et al., *Application of a Physiologically Based Pharmacokinetic Model for Isopropanol in the Derivation of a Reference Dose and Reference Concentration.* Regulatory Toxicology and Pharmacology, 2002. **36**(1): p. 51-68.

54. Martin, S.A., et al., *Development of multi-route physiologically-based pharmacokinetic models for ethanol in the adult, pregnant, and neonatal rat.* Inhalation Toxicology, 2012. **24**(11): p. 698-722.

55. You, L., et al., *Transplacental and Lactational Transfer of p,p'-DDE in Sprague–Dawley Rats.* Toxicology and Applied Pharmacology, 1999. **157**(2): p. 134-144.

56. ICRP, *Basic Anatomical and Physiological Data for Use in Radiological Protection Reference Values.* Vol. 32. 2002: ICRP Publication 89. Ann. .

57. O'Flaherty, E.J., et al., *A physiologically based kinetic model of rat and mouse gestation: Disposition of a weak acid.* Toxicology and Applied Pharmacology, 1992. **112**(2): p. 245-256.

58. Clarke, D.O., et al., *Pharmacokinetics of 2-Methoxyethanol and 2-Methoxyacetic Acid in the Pregnant Mouse: A Physiologically Based Mathematical Model.* Toxicology and Applied Pharmacology, 1993. **121**(2): p. 239-252.

59. Terry, K.K., et al., *Development of a Physiologically Based Pharmacokinetic Model Describing 2-Methoxyacetic Acid Disposition in the Pregnant Mouse.* Toxicology and Applied Pharmacology, 1995. **132**(1): p. 103-114.

60. Kawamoto, Y., et al., *Development of a physiologically based pharmacokinetic model for bisphenol A in pregnant mice.* Toxicology and Applied Pharmacology, 2007. **224**(2): p. 182-191.

61. Clewell, R.A., et al., *Tissue Exposures to Free and Glucuronidated Monobutylyphthalate in the Pregnant and Fetal Rat following Exposure to Di-n-butylphthalate: Evaluation with a PBPK Model.* Toxicological Sciences, 2008. **103**(2): p. 241-259.

62. Yoon, M., et al., *Evaluating Placental Transfer and Tissue Concentrations of Manganese in the Pregnant Rat and Fetuses after Inhalation Exposures with a PBPK Model.* Toxicological Sciences, 2009. **112**(1): p. 44-58.

63. Loccisano, A.E., et al., *Evaluation of placental and lactational pharmacokinetics of PFOA and PFOS in the pregnant, lactating, fetal and neonatal rat using a physiologically based pharmacokinetic model.* Reproductive Toxicology, 2012. **33**(4): p. 468-490.

64. Takaku, T., H. Nagahori, and Y. Sogame, *Metabolism and physiologically based pharmacokinetic modeling of flumioxazin in pregnant animals.* Toxicology and Applied Pharmacology, 2014. **277**(3): p. 242-249.

65. Clewell, R.A., et al., *Predicting Fetal Perchlorate Dose and Inhibition of Iodide Kinetics during Gestation: A Physiologically-Based Pharmacokinetic Analysis of Perchlorate and Iodide Kinetics in the Rat.* Toxicological Sciences, 2003. **73**(2): p. 235-255.

66. Buelke-Sam, J., et al., *Blood flow during pregnancy in the rat: I. Flow patterns to maternal organs.* Teratology, 1982. **26**(3): p. 269-277.

67. Buelke-Sam, J., H.J. F., and C.J. Nelson, *Blood flow during pregnancy in the rat: II. Dynamics of and litter variability in uterine flow.* Teratology, 1982. **26**(3): p. 279-288.

68. Xia, B., et al., *A simplified PBPK modeling approach for prediction of pharmacokinetics of four primarily renally excreted and CYP3A metabolized compounds during pregnancy.* Journal of the American Association of Pharmaceutical Scientists, 2013. **15**(4): p. 1012-1024.

69. Alqahtani, S. and A. Kaddoumi, *Development of Physiologically Based Pharmacokinetic/Pharmacodynamic Model for Indomethacin Disposition in Pregnancy.* PLOS ONE, 2015. **10**(10): p. e0139762.

70. De Sousa Mendes, M., et al., *A Physiologically-Based Pharmacokinetic Model to Predict Human Fetal Exposure for a Drug Metabolized by Several CYP450 Pathways.* Clinical Pharmacokinetics, 2017. **56**(5): p. 537-550.

71. Verner, M.-A., et al., *Physiologically based pharmacokinetic modeling of persistent organic pollutants for lifetime exposure assessment: a new tool in breast cancer epidemiologic studies.* Environmental health perspectives, 2008. **116**(7): p. 886-892.

72. Poet, T.S., et al., *Quantitative Risk Analysis for N-Methyl Pyrrolidone Using Physiologically Based Pharmacokinetic and Benchmark Dose Modeling.* Toxicological Sciences, 2010. **113**(2): p. 468-482.

73. Sharma, R.P., M. Schuhmacher, and V. Kumar, *The development of a pregnancy PBPK Model for Bisphenol A and its evaluation with the available biomonitoring data.* Science of The Total Environment, 2018. **624**: p. 55-68.

74. Verner, M.-A., et al., *Associations of Perfluoroalkyl Substances (PFAS) with Lower Birth Weight: An Evaluation of Potential Confounding by Glomerular Filtration Rate Using a Physiologically Based Pharmacokinetic Model (PBPK).* Environmental health perspectives, 2015. **123**(12): p. 1317-1324.

75. Yoon, M., et al., *Physiologically Based Pharmacokinetic Modeling of Fetal and Neonatal Manganese Exposure in Humans: Describing Manganese Homeostasis during Development.* Toxicological Sciences, 2011. **122**(2): p. 297-316.

76. Kiserud, T., et al., *Fetal cardiac output, distribution to the placenta and impact of placental compromise.* Ultrasound in Obstetrics & Gynecology, 2006. **28**(2): p. 126-136.

77. Valcke, M. and K. Krishnan, *Evaluation of the impact of the exposure route on the human kinetic adjustment factor.* Regulatory Toxicology and Pharmacology, 2011. **59**(2): p. 258-269.

78. Luecke, R.H., et al., *A physiologically based pharmacokinetic computer model for human pregnancy.* Teratology, 1994. **49**(2): p. 90-103.

79. Gray, D.G., *A Physiologically Based Pharmacokinetic Model for Methyl Mercury in the Pregnant Rat and Fetus.* Toxicology and Applied Pharmacology, 1995. **132**(1): p. 91-102.

80. Sweeney, L.M., et al., *Development of a physiologically based pharmacokinetic (PBPK) model for methyl iodide in rats, rabbits, and humans.* Inhalation Toxicology, 2009. **21**(6): p. 552-582.

81. Rudolph Abraham, M. and A. Heymann Michael, *The Circulation of the Fetus in Utero.* Circulation Research, 1967. **21**(2): p. 163-184.

82. Lorijn, R.H., J.C. Nelson, and L.D. Longo, *Induced fetal hyperthyroidism: cardiac output and oxygen consumption.* American Journal of Physiology-Heart and Circulatory Physiology, 1980. **239**(3): p. H302-H307.

83. Kim, C.S., Z. Binienda, and J.A. Sandberg, *Construction of a Physiologically Based Pharmacokinetic Model for 2,4-Dichlorophenoxyacetic Acid Dosimetry in the Developing Rabbit Brain.* Toxicology and Applied Pharmacology, 1996. **136**(2): p. 250-259.

84. Flo, K., T. Wilsgaard, and G. Acharya, *Longitudinal reference ranges for umbilical vein blood flow at a free loop of the umbilical cord.* Ultrasound in Obstetrics & Gynecology, 2010. **36**(5): p. 567-572.

85. Haugen, G., et al., *Portal and umbilical venous blood supply to the liver in the human fetus near term.* Ultrasound in Obstetrics & Gynecology, 2004. **24**(6): p. 599-605.

86. Ward, K.W., et al., *Development of a Physiologically Based Pharmacokinetic Model to Describe the Disposition of Methanol in Pregnant Rats and Mice.* Toxicology and Applied Pharmacology, 1997. **145**(2): p. 311-322.

87. Strikwold, M., et al., *Integrating in vitro data and physiologically based kinetic (PBK) modelling to assess the in vivo potential developmental toxicity of a series of phenols.* Archives of toxicology, 2017. **91**(5): p. 2119-2133.

88. Horton, S., et al., *Maximum Recommended Dosage of Lithium for Pregnant Women Based on a PBPK Model for Lithium Absorption.* Advances in bioinformatics, 2012. **2012**: p. 352729.

89. Dallmann, A., et al., *Physiologically Based Pharmacokinetic Modeling of Renally Cleared Drugs in Pregnant Women.* Clinical Pharmacokinetics, 2017. **56**(12): p. 1525-1541.

90. Geraghty, A.A., et al., *Maternal and fetal blood lipid concentrations during pregnancy differ by maternal body mass index: findings from the ROLO study.* BMC pregnancy and childbirth, 2017. **17**(1): p. 360-360.

91. Clewell, H.J., et al., *Evaluation of the Uncertainty in an Oral Reference Dose for Methylmercury Due to Interindividual Variability in Pharmacokinetics.* Risk Analysis, 1999. **19**(4): p. 547-558.

92. Schmitt, W., *General approach for the calculation of tissue to plasma partition coefficients.* Toxicology in Vitro, 2008. **22**(2): p. 457-467.

93. Poulin, P., K. Schoenlein, and F.P. Theil, *Prediction of adipose tissue: Plasma partition coefficients for structurally unrelated drugs.* Journal of Pharmaceutical Sciences, 2001. **90**(4): p. 436-447.

94. Poulin, P. and F.P. Theil, *A Priori Prediction of Tissue:Plasma Partition Coefficients of Drugs to Facilitate the Use of Physiologically‐Based Pharmacokinetic Models in Drug Discovery.* Journal of Pharmaceutical Sciences, 2000. **89**(1): p. 16-35.

95. Giaginis, C., et al., *Application of quantitative structure–activity relationships for modeling drug and chemical transport across the human placenta barrier: a multivariate data analysis approach.* Journal of Applied Toxicology, 2009. **29**(8): p. 724-733.

96. Hewitt, M., et al., *Structure-based modelling in reproductive toxicology: (Q)SARs for the placental barrier.* SAR and QSAR in Environmental Research, 2007. **18**(1-2): p. 57-76.

97. Lu, F., et al., *Prediction of placenta barrier permeability and reproductive toxicity of compounds in tocolytic Chinese herbs using support vector machine*, in *International Conference on Materials Engineering and Information Technology Applications*. 2015, Atlantis Press. p. 650-655.

98. Zhang, Y.-H., et al., *Prediction of Placental Barrier Permeability: A Model Based on Partial Least Squares Variable Selection Procedure.* Molecules, 2015. **20**: p. 8270-8286.

99. Eguchi, A., et al., *Maternal–fetal transfer rates of PCBs, OCPs, PBDEs, and dioxin-like compounds predicted through quantitative structure–activity relationship modeling.* Environmental Science and Pollution Research, 2018. **25**(8): p. 7212-7222.

100. Takaku, T., et al., *Quantitative Structure–Activity Relationship Model for the Fetal–Maternal Blood Concentration Ratio of Chemicals in Humans.* Biological and Pharmaceutical Bulletin, 2015. **38**(6): p. 930-934.

101. Kovo, M. and A. Golan, *In Vitro Models Using the Human Placenta to Study Fetal Exposure to Drugs.* Clinical medicine. Reproductive health, 2008. **2**: p. 15-24.

102. Evseenko, D.A., J.W. Paxton, and J.A. Keelan, *ABC drug transporter expression and functional activity in trophoblast-like cell lines and differentiating primary trophoblast.* American Journal of Physiology-Regulatory, Integrative and Comparative Physiology, 2006. **290**(5): p. R1357-R1365.

103. Liu, F., M.J. Scares, and K.L. Audus, *Permeability and biochemical properties of BeWo trophoblast cell monolayers.* Placenta, 1996. **17**(5): p. A25.

104. Li, H., et al., *Assessment of an in vitro transport model using BeWo b30 cells to predict placental transfer of compounds.* Archives of Toxicology, 2013. **87**(9): p. 1661-1669.

105. Poulsen, M.S., et al., *Modeling placental transport: Correlation of in vitro BeWo cell permeability and ex vivo human placental perfusion.* Toxicology in Vitro, 2009. **23**(7): p. 1380-1386.

106. Aengenheister, L., et al., *An advanced human in vitro co-culture model for translocation studies across the placental barrier.* Scientific Reports, 2018. **8**(1): p. 5388.

107. Lee, J., et al., *Placenta-on-a-chip: a novel platform to study the biology of the human placenta.* The Journal of Maternal-Fetal & Neonatal Medicine, 2016. **29**(7): p. 1046-1054.

108. Blundell, C., et al., *A microphysiological model of the human placental barrier.* Lab on a chip, 2016. **16**(16): p. 3065-3073.

109. Yin, F., et al., *A 3D human placenta-on-a-chip model to probe nanoparticle exposure at the placental barrier.* Toxicology in Vitro, 2019. **54**: p. 105-113.

110. Huang, X., et al., *Establishment of a confluent monolayer model with human primary trophoblast cells: novel insights into placental glucose transport.* MHR: Basic science of reproductive medicine, 2016. **22**(6): p. 442-456.

111. Kallol, S., et al., *Novel Insights into Concepts and Directionality of Maternal–Fetal Cholesterol Transfer across the Human Placenta.* International Journal of Molecular Sciences, 2018. **19**(8).

112. Zhang, Z. and J.D. Unadkat, *Verification of a Maternal-Fetal Physiologically Based Pharmacokinetic Model for Passive Placental Permeability Drugs.* Drug Metabolism and Disposition, 2017: p. dmd.116.073957.

113. Varma, D.R. and R. Ramakrishnan, *A rat model for the study of transplacental pharmacokinetics and its assessment with antipyrine and aminoisobutyric acid.* Journal of Pharmacological Methods, 1985. **14**(1): p. 61-74.

114. Kanto, J., et al., *Placental transfer and maternal midazolam kinetics.* Clinical Pharmacology & Therapeutics, 1983. **33**(6): p. 786-791.

115. Panigel, M., *Placental perfusion experiments.* American Journal of Obstetrics and Gynecology, 1962. **84**(11, Part 2): p. 1664-1683.

116. Miller, R.K., et al., *Human Placenta in vitro: Characterization during 12 h of Dual Perfusion*, in *In vitro Perfusion of Human Placental Tissue*, H. Schneider and J. Dancis, Editors. 1985: Zürich. p. 77-84.

117. Schneider, H., et al., *Evaluation of an In Vitro Dual Perfusion System for the Study of Placental Proteins: Energy Metabolism*, in *Placenta as a Model and a Source*, O. Genbačev, A. Klopper, and R. Beaconsfield, Editors. 1989, Springer US: Boston, MA. p. 39-50.

118. Ala-Kokko, T.I., P. Myllynen, and K. Vähäkangas, *Ex vivo perfusion of the human placental cotyledon: implications for anesthetic pharmacology.* International Journal of Obstetric Anesthesia, 2000. **9**(1): p. 26-38.

119. Hutson, J.R., et al., *The Human Placental Perfusion Model: A Systematic Review and Development of a Model to Predict In Vivo Transfer of Therapeutic Drugs.* Clinical Pharmacology & Therapeutics, 2011. **90**(1): p. 67-76.

120. Heikkinen, T., U. Ekblad, and K. Laine, *Transplacental transfer of citalopram, fluoxetine and their primary demethylated metabolites in isolated perfused human placenta.* BJOG: An International Journal of Obstetrics & Gynaecology, 2002. **109**(9): p. 1003-1008.

121. Julius, J.M., et al., *Evaluation of the maternal–fetal transfer of granisetron in an ex vivo placenta perfusion model.* Reproductive Toxicology, 2014. **49**: p. 43-47.

122. Jovelet, C., et al., *Variation in transplacental transfer of tyrosine kinase inhibitors in the human perfused cotyledon model.* Annals of Oncology, 2015. **26**(7): p. 1500-1504.

123. Vinot, C., et al., *Bidirectional Transfer of Raltegravir in an Ex Vivo Human Cotyledon Perfusion Model.* Antimicrobial agents and chemotherapy, 2016. **60**(5): p. 3112-3114.

124. Mandelbrot, L., et al., *Placental transfer of rilpivirine in an ex vivo human cotyledon perfusion model.* Antimicrobial agents and chemotherapy, 2015. **59**(5): p. 2901-2903.

125. Freriksen, J.J.M., et al., *Placental disposition of the immunosuppressive drug tacrolimus in renal transplant recipients and in ex vivo perfused placental tissue.* European Journal of Pharmaceutical Sciences, 2018. **119**: p. 244-248.

126. Shintaku, K., et al., *Prediction and evaluation of fetal toxicity induced by NSAIDs using transplacental kinetic parameters obtained from human placental perfusion studies.* British journal of clinical pharmacology, 2012. **73**(2): p. 248-256.

127. Schalkwijk, S., et al., *Prediction of Fetal Darunavir Exposure by Integrating Human Ex-Vivo Placental Transfer and Physiologically Based Pharmacokinetic Modeling.* Clinical pharmacokinetics, 2018. **57**(6): p. 705-716.

128. Fisher, J.W., et al., *Physiologically based pharmacokinetic modeling of the pregnant rat: A multiroute exposure model for trichloroethylene and its metabolite, trichloroacetic acid.* Toxicology and Applied Pharmacology, 1989. **99**(3): p. 395-414.

129. Emond, C., et al., *A physiologically based pharmacokinetic model for developmental exposure to BDE-47 in rats.* Toxicology and Applied Pharmacology, 2010. **242**(3): p. 290-298.

130. Emond, C., et al., *An assessment of dioxin exposure across gestation and lactation using a PBPK model and new data from Seveso.* Environment international, 2016. **92-93**: p. 23-32.

131. Han, L.W., C. Gao, and Q. Mao, *An update on expression and function of P-gp/ABCB1 and BCRP/ABCG2 in the placenta and fetus.* Expert Opinion on Drug Metabolism & Toxicology, 2018. **14**(8): p. 817-829.

132. Challier, J.C., *La barrière placentaire : structure, résistance, asymétrie*. Reproduction Nutrition Development. Vol. 29. 1989. 703-716.

133. Dahl Andersen, M., et al., *Animal Models of Fetal Medicine and Obstetrics*, in *Experimental Animal Models of Human Diseases - An Effective Therapeutic Strategy*. 2018.

134. Hirt, D., et al., *Pharmacokinetic modelling of the placental transfer of nelfinavir and its M8 metabolite: a population study using 75 maternal-cord plasma samples.* British Journal of Clinical Pharmacology, 2007. **64**(5): p. 634-644.

135. Shapiro, G.D., et al., *Exposure to organophosphorus and organochlorine pesticides, perfluoroalkyl substances, and polychlorinated biphenyls in pregnancy and the association with impaired glucose tolerance and gestational diabetes mellitus: The MIREC Study.* Environmental Research, 2016. **147**: p. 71-81.

136. Lignell, S., et al., *Maternal body burdens of PCDD/Fs and PBDEs are associated with maternal serum levels of thyroid hormones in early pregnancy: a cross-sectional study.* Environmental health, 2016. **15**: p. 55-55.

137. Andra, S.S., C. Austin, and M. Arora, *Tooth matrix analysis for biomonitoring of organic chemical exposure: Current status, challenges, and opportunities.* Environmental research, 2015. **142**: p. 387-406.

138. Tsatsakis, A.M., et al., *Dialkyl phosphates in meconium as a biomarker of prenatal exposure to organophosphate pesticides: A study on pregnant women of rural areas in Crete, Greece.* Xenobiotica, 2009. **39**(5): p. 364-373.

139. Koutroulakis, D., et al., *Dialkyl phosphates in amniotic fluid as a biomarker of fetal exposure to organophosphates in Crete, Greece; association with fetal growth.* Reproductive Toxicology, 2014. **46**: p. 98-105.

140. Wan, Y., et al., *Hydroxylated Polybrominated Diphenyl Ethers and Bisphenol A in Pregnant Women and Their Matching Fetuses: Placental Transfer and Potential Risks.* Environmental Science & Technology, 2010. **44**(13): p. 5233-5239.

141. Cao, X.-L., et al., *Bisphenol A in human placental and fetal liver tissues collected from Greater Montreal area (Quebec) during 1998–2008.* Chemosphere, 2012. **89**(5): p. 505-511.

142. Needham, L.L., et al., *Partition of environmental chemicals between maternal and fetal blood and tissues.* Environmental science & technology, 2011. **45**(3): p. 1121-1126.

143. Mandy, M. and M. Nyirenda, *Developmental Origins of Health and Disease: the relevance to developing nations.* International health, 2018. **10**(2): p. 66-70.

144. Kapraun, D.F., et al., *Empirical models for anatomical and physiological changes in a human mother and fetus during pregnancy and gestation.* PloS one, 2019. **14**(5): p. e0215906-e0215906.

145. Mölsä, M., et al., *Functional role of P-glycoprotein in the human blood-placental barrier.* Clinical Pharmacology & Therapeutics, 2005. **78**(2): p. 123-131.

146. Gluzman, B.E. and H. Niepomniszcze, *Kinetics of the iodide trapping mechanism in normal and pathological human thyroid slices.* Acta Endocrinologica, 1983. **103**(1): p. 34-39.

147. Wolff, J. and J.R. Walrey, *Thyroidal iodide transport: IV. The role of ion size.* Biochimica et Biophysica Acta, 1963. **69**: p. 58-67.

148. De Sousa Mendes, M., et al., *Prediction of human fetal pharmacokinetics using ex vivo human placenta perfusion studies and physiologically based models.* British journal of clinical pharmacology, 2016. **81**(4): p. 646-657.

149. Ring, A., et al., *Hepatic Maturation of Human Fetal Hepatocytes in Four-Compartment Three-Dimensional Perfusion Culture.* Tissue Engineering Part C: Methods, 2009. **16**(5): p. 835-845.

150. Abdul Naveed Shaik, S.K.V., Aleem A Khan, *Metabolism of six CYP probe substrates in fetal hepatocytes.* ADMET & DMPK, 2016.

151. Bouazza, N., et al., *Methodological Approaches To Evaluate Fetal Drug Exposure.* Curr Pharm Des, 2019. **25**: p. 1-1.

152. Saghir, S.A., S.A. Khan, and A.T. McCoy, *Ontogeny of mammalian metabolizing enzymes in humans and animals used in toxicological studies.* Critical Reviews in Toxicology, 2012. **42**(5): p. 323-357.

153. Dallmann, A., et al., *Drug Transporters Expressed in the Human Placenta and Models for Studying Maternal-Fetal Drug Transfer.* The Journal of Clinical Pharmacology, 2019. **59**(S1): p. S70-S81.

154. Berveiller, P., et al., *Drug transporter expression during in vitro differentiation of first-trimester and term human villous trophoblasts.* Placenta, 2015. **36**(1): p. 93-96.

155. Bell, S.M., et al., *In vitro to in vivo extrapolation for high throughput prioritization and decision making.* Toxicology in Vitro, 2018. **47**: p. 213-227.

156. Jensen, O.E. and I.L. Chernyavsky, *Blood Flow and Transport in the Human Placenta.* Annual Review of Fluid Mechanics, 2019. **51**(1): p. 25-47.

157. Olanoff, L. and J. Anderson, *Controlled release of tetracycline—III: A physiological pharmacokinetic model of the pregnant rat.* Journal of Pharmacokinetics and Biopharmaceutics, 1980. **8**(6): p. 599-620.

158. Gentry, P.R., T.R. Covington, and H.J. Clewell, *Evaluation of the potential impact of pharmacokinetic differences on tissue dosimetry in offspring during pregnancy and lactation.* Regulatory Toxicology and Pharmacology, 2003. **38**(1): p. 1-16.

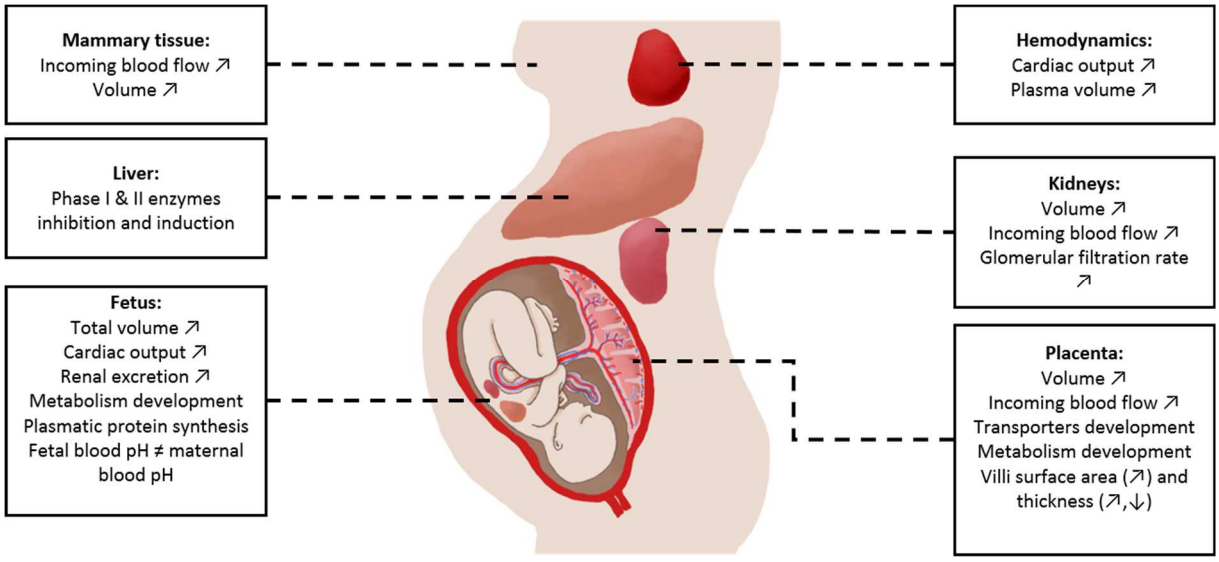

Figure 1: Physiological, anatomical and biochemical changes in the mother and the fetus which could influence maternal or fetal dosimetry [9, 10].

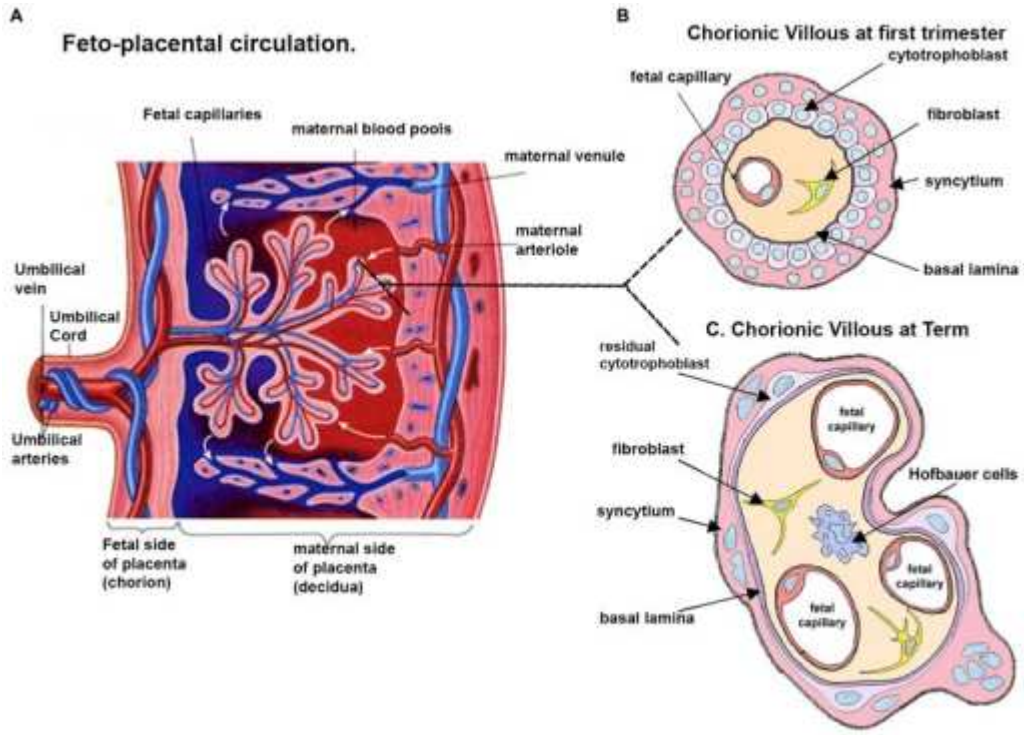

Figure 2: Schematic representation of the human placental organization. (A) Fetal placental circulation structure after the first trimester of pregnancy. The placental thickness at full term is approximately 2.5 cm [156]. The dotted lines show the position from which drawings of a section through the chorionic villous are taken at ~10 weeks (B) and term (C). (B) Chorionic villous inner part at the end of the first trimester. (C) Chorionic villous inner part at term. Source (10.3389/fphar.2014.00133.), license CC BY 3.0.

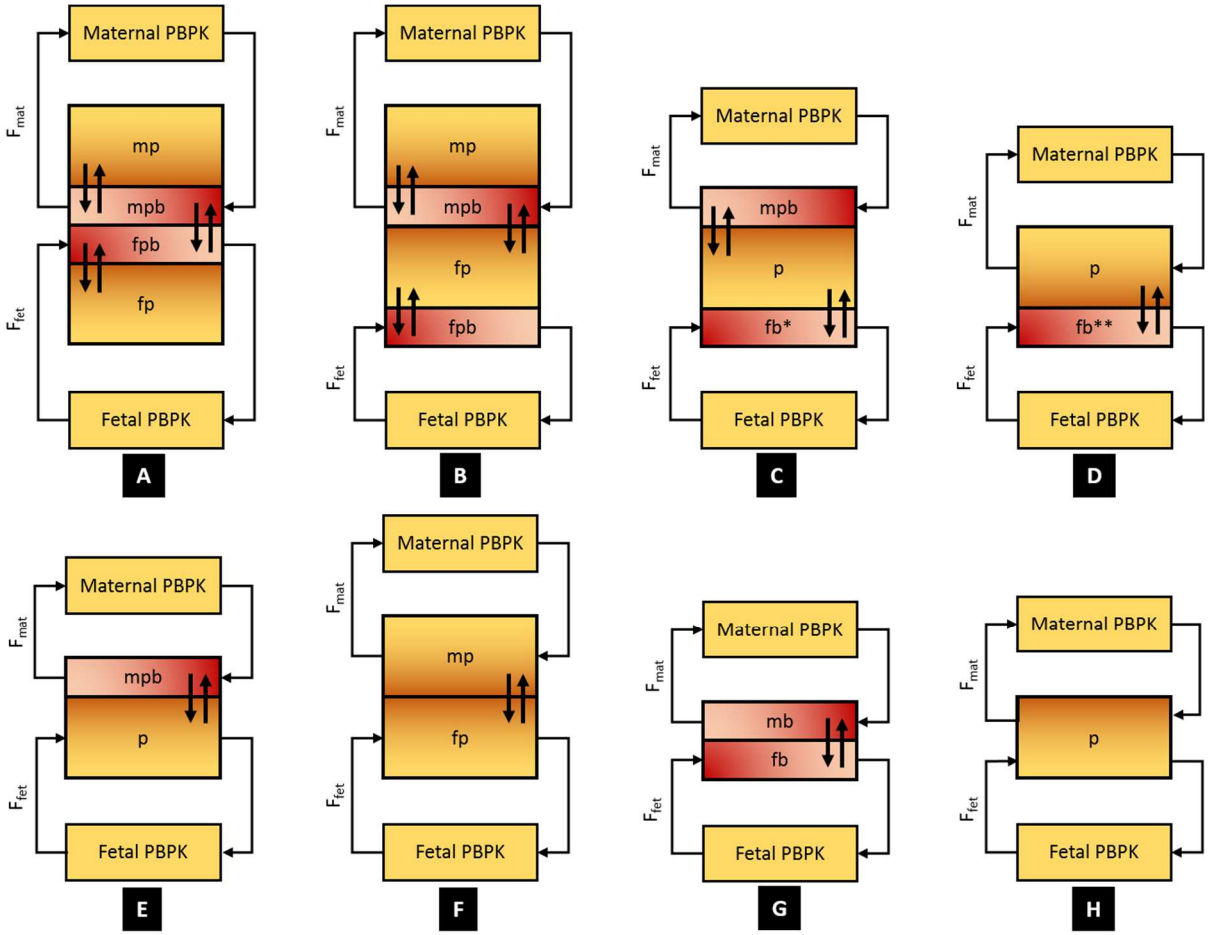

Figure 3: Classes of placental transfer structures for models with a fetal PBPK sub-model (group 1). The yellow compartments represent a maternal or a fetal PBPK sub-model. The yellow-red gradient boxes represent the placental tissue compartments. The pink-red gradient boxes represent blood compartments. The symbols *mb, fb, mp, mpb, fpb, fp* and *p* refer to maternal blood, fetal blood, maternal placenta, maternal placental blood, fetal placental blood, fetal placenta and placenta, respectively. F_{mat} and F_{fet} represent maternal and fetal blood flows to placenta, respectively. C_{blood} and $C_{bloodfet}$ refer to maternal and fetal blood concentrations, respectively. The arrows which do not represent the blood flows consider diffusions. **fpb* in Zhang et al. (2017). ***fpb* in Andrew et al. (2008).

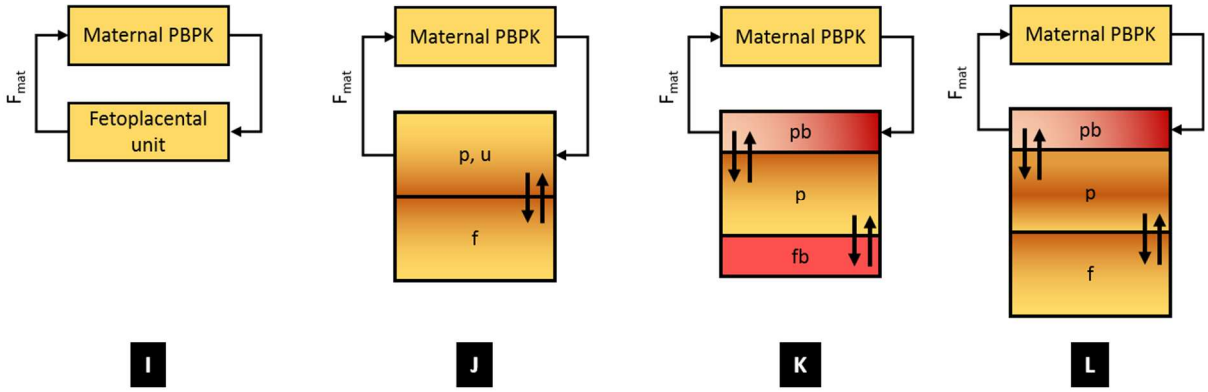

1209

1210 **Figure 4:** Classes of placental transfer structures for models without a fetal PBPK sub-model
1211 (group 2). The yellow-red gradient boxes represent the tissue compartments. The red boxes
1212 represent blood compartments. The symbols *p, u, f, pb* and *fb* refer to placenta, uterus, fetus,
1213 placental blood and fetal blood, respectively. F_{mat} represents the maternal blood flow to
1214 placenta, respectively. C_{blood} and $C_{bloodfet}$ refer to the maternal blood concentration, respectively.
1215 The arrows which do not represent the blood flows consider diffusions.

1216

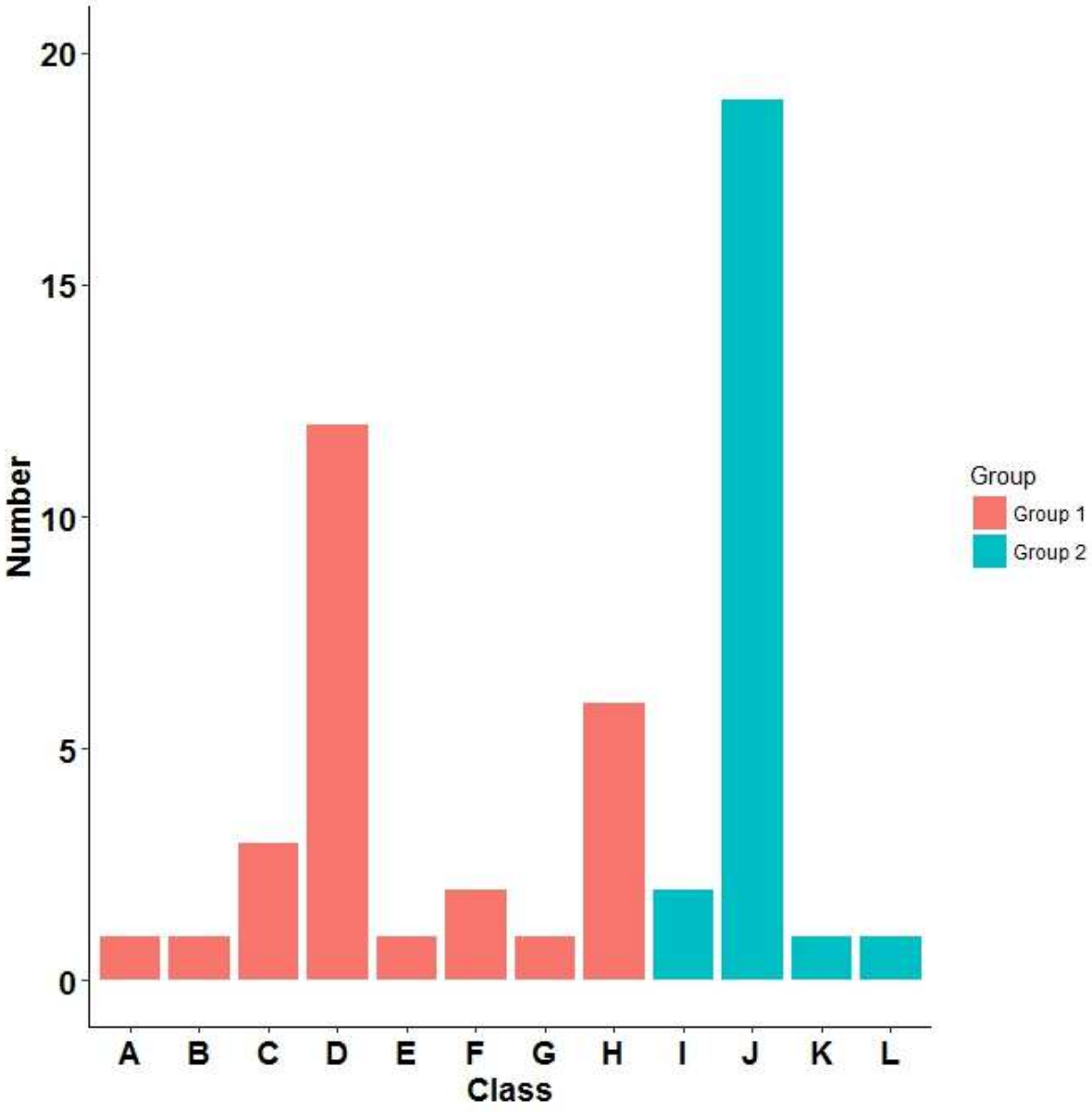

Figure 5: Bar plot of the different structure classes for placental transfer in pPBPK models.

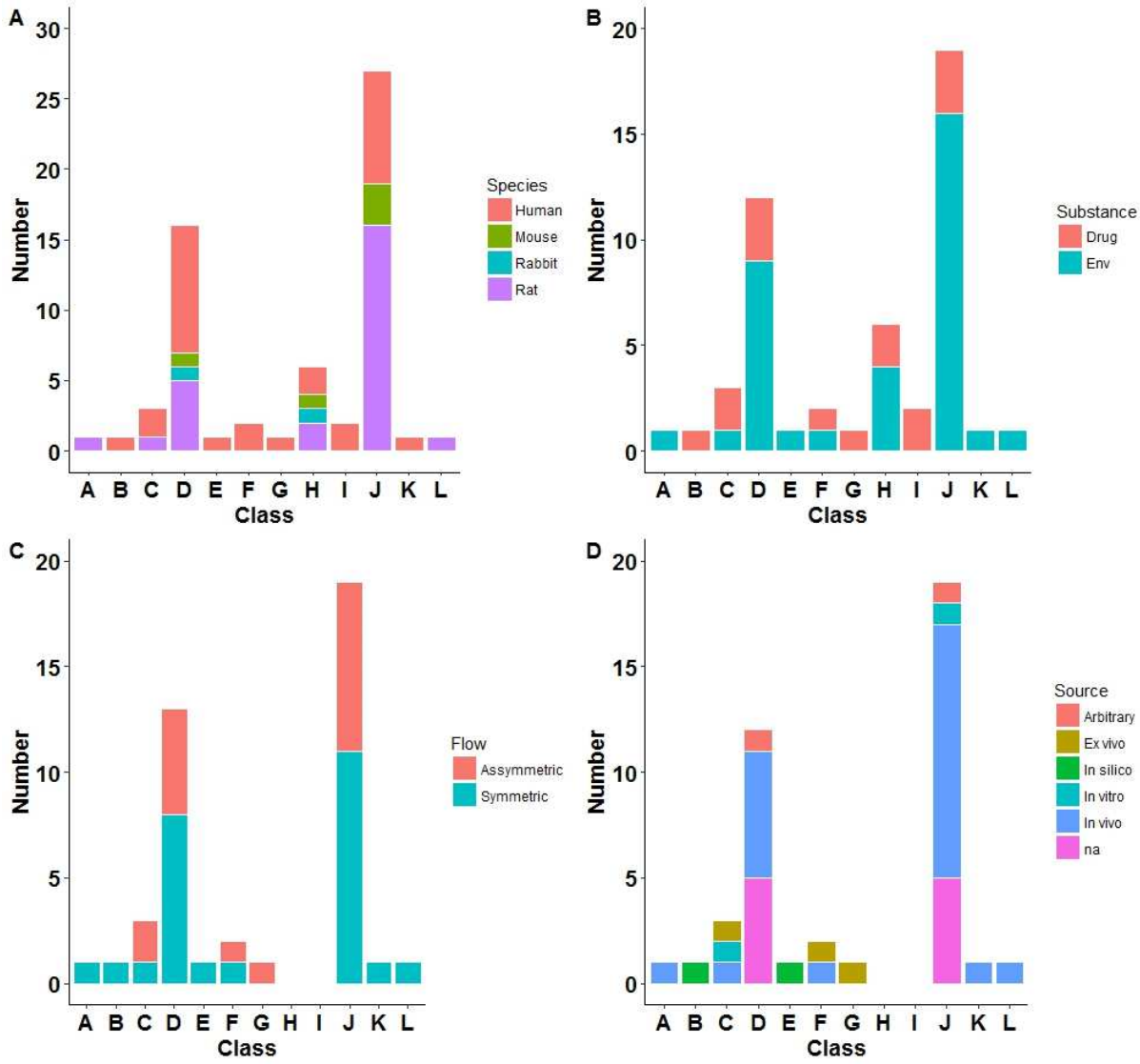

Figure 6: Bar plots of the different structure classes for placental transfer according to (A) species encountered in pPBPK models. A model developed for two or three species is counted two and three times respectively. (B) the type of substances encountered in p-PBPK models. "Env" stands for environmental pollutant. (C) the value setting of the placental diffusion parameters in opposite direction. Models belonging to class H and I were not included since they were flow-limited placental transfer structures. Loccisano et al. (2013) was included twice since the placental diffusion transfer was symmetric for perfluorooctanoic acid (PFOA) and asymmetric for perfluorooctane sulfonate (PFOS). (D) the source of information for placental

diffusion parameters parameterization. Models belonging to class H and I were not included since they were flow-limited placental transfer structures.

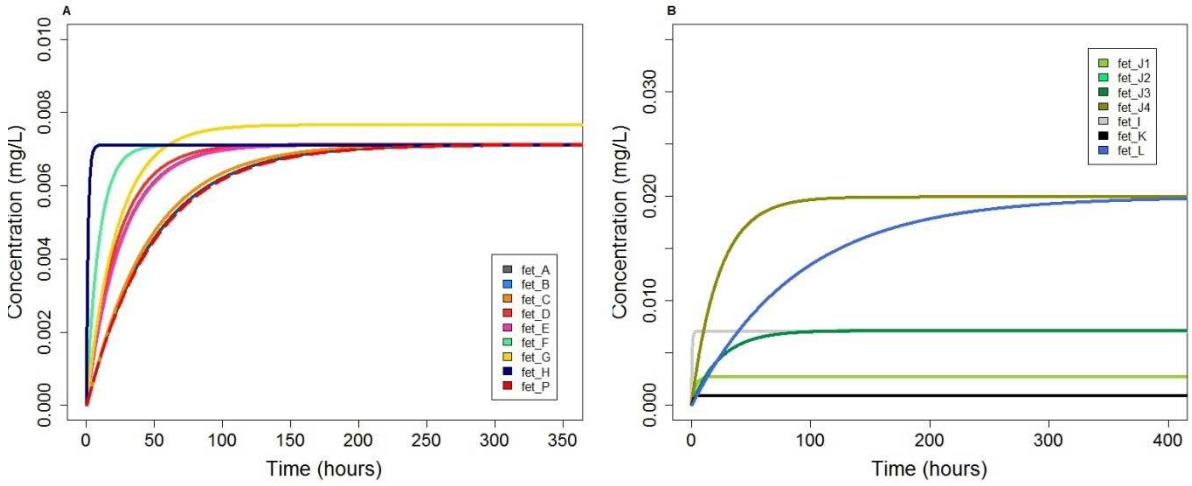

1232

1233 **Figure 7**: Simulated fetal concentrations (A) from group 1 models (Fetal PBPK

1234 compartment); (B) from group 2 models (Fetoplacental unit, f and fb compartments). The

1235 legend fet_X corresponds to the predictions obtained with the class X model.

1236

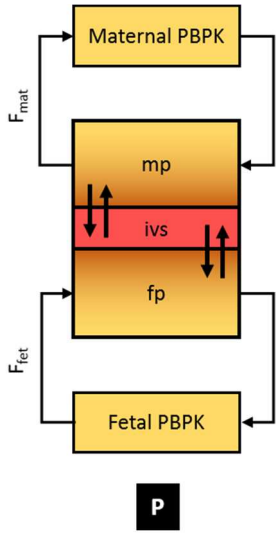

Figure 8: Class P model placental transfer structure (early phase). The yellow compartments represent a maternal or a fetal PBPK sub-model. The yellow-red gradient boxes represent the placental tissue compartments. The red box represent blood in the intervillous space. The symbols *mp*, *fp* and *ivs* refer to maternal and fetal placenta and intervillous space, respectively. F_{mat} and F_{fet} represent maternal and fetal blood flows to placenta, respectively. C_{blood} and $C_{bloodfet}$ refer to maternal and fetal blood concentrations, respectively. The arrows which do not represent the blood flows consider diffusions.

Table 1: Placental transfer structures'classes in group 1 models and diffusion apparent transfer parameterizations.

First author	Year	Subst. Nature	Species	Class	Passive diffusion parameter						Reference
					Sym	fBW	mBW	plaW	exchS	Source	
Olanoff	1980	Drug	Rat	H	-	-	-	-	-	-	[157]
Fisher*	1989	Env	Rat	H	-	-	-	-	-	-	[128]
O'Flaherty	1992	Drug	Rat/mouse	D	y	n	y	n	n	arbitrary	[57]
Luecke	1994	Drug	Human	D	y	n	n	y	n	na	[78]
Gray**	1995	Env	Rat	A	y	n	n	y	n	animal *in vivo*	[79]
Terry	1995	Env	Mouse	H	-	-	-	-	-	-	[59]
Kim	1996	Env	Rabbit	H	-	-	-	-	-	-	[83]
Clewell	1999	Env	Human	D	y	n	y	n	n	animal/human *in vivo*	[91]
Clewell**	2003	Env	Rat	C	n	n	y	n	n	animal *in vivo*	[65]
Gentry	2003	Env	Human	D	y	y	n	n	n	na	[158]
Andrew	2008	Drug	Human	D	y	n	n	n	n	na	[7]
Sweeney	2009	Env	Rat/rabbit/human	D	n	n	y	n	n	animal and human *in vivo*	[80]
Beaudouin	2010	Env	Human	F	y	n	n	n	n	human *in vivo* (%mBF)	[8]
Valcke	2011	Env	Human	H	-	-	-	-	-	-	[77]
Yoon	2011	Env	Rat/human	D	y	y	n	n	n	arbitrary	[75]
Shintaku**	2011	Drug	Human	C	n	n	n	n	n	*ex vivo*	[126]
Loccisano	2012	Env	Rat	D	n	y	n	n	n	animal *in vivo*	[63]
Horton	2012	Drug	Human	H	-	-	-	-	-	-	[88]
Loccisano	2013	Env	Human	D	PFOA: y / PFOS: n	y	n	n	n	human *in vivo*	[51]
Lumen	2013	Env	Human	E	y	n	y	n	n	model calibration	[40]
Martin	2014	Env	Rat	D	y	y	n	n	n	animal *in vivo*	[49]
Verner	2015	Env	Human	D	n	y	n	n	n	na	[74]
De Sousa Mendes	2016	Drug	Human	F	n	n	n	y	n	*ex vivo*	[70]
Sharma	2017	Env	Human	D	n	y	n	n	n	animal *in vivo*	[73]
Dallmann**	2017	Drug	Human	B	y	n	n	n	y	semi-empirical equation	[89]
Zhang**	2017	Drug	Human	C	y	n	n	n	y	human *in vivo*/*in vitro*	[112]
Schalkwijk	2017	Drug	Human	G	n	n	n	n	n	*ex vivo*	[127]

y = yes; **n** = no; **Subst.nature** = substance nature; **Sym** = symmetrical; **fBW** = proportional to fetal bodyweight; **mBW** = proportional to maternal bodyweight; **plaW** = proportional to placental weight; **exchS** = proportional to surface of exchange; **Source** = source of information; **mBF** = maternal blood flow to placenta. *For trichloroethylene (TCE). **The considered passive diffusion parameter is set between maternal placental blood (or plasma, as in the following) and fetal placental blood (or plasma, as in the following) in Gray et al., between placenta and fetal

plasma in Clewell et al., between maternal placental blood and placenta and between placenta and fetal placental blood in Shintaku et al., between maternal placental blood and fetal placenta in Dallmann et al., between placenta and fetal placental blood in Zhang et al. The notifications placental, maternal or fetal blood are generic and correspond to Figure 3 compartment notifications.

Table 2: Placental transfer structures'classes in group 2 models and diffusion apparent transfer parameterizations.

					Passive diffusion parameter				
First author	**Year**	**Subst. Nature**	**Species**	**Class**	**Sym**	**fBW**	**mBW**	**Source**	**Reference**
Gabrielsson	1983	Drug	Rat/human	J	y	n	n	na	[41]
Gabrielsson	1984	Drug	Rat/human	J	y	n	n	animal *in vivo*	[42]
Gabrielsson	1986	Drug	Rat/human	J	y	n	n	na	[43]
Fisher*	1989	Env	Rat	J	n	n	n	animal *in vivo*	[128]
Clarke	1993	Env	Mouse	J	n	n	n	animal *in vivo*	[58]
Ward	1997	Env	Rat/mouse	J	n	n	n	animal *in vivo*	[86]
You	1999	Env	Rat	J	n	n	n	animal *in vivo*	[55]
Gentry	2002	Env	Rat/human	J	y	y	n	na	[53]
Emond**	2004	Env	Rat	L	y	n	n	animal *in vivo*	[48]
Kawamoto	2007	Env	Rat	J	n	n	n	na	[60]
Clewell**	2007	Env	Human	K	y	n	y	human *in vivo*	[47]
Verner	2008	Env	Rat/human	J	y	y	n	arbitrary	[71]
Clewell	2008	Env	Rat	J	y	y	n	animal *in vivo*	[61]
Emond	2010	Env	Rat	J	y	n	n	animal *in vivo*	[129]
Poet	2010	Env	Rat/human	J	y	y	n	arbitrary	[72]
Martin	2012	Env	Rat	J	y	y	n	animal *in vivo*	[54]
Gaohua	2012	Drug	Human	I	-	-	-	-	[45]
Lin	2013	Env	Rat	J	n	y	n	animal *in vivo*	[50]
Crowell	2013	Env	Mouse	J	n	n	n	animal *in vivo*	[46]
Takaku	2014	Env	Rat/human	J	n	n	n	animal *in vivo*	[64]
Alqahtani	2015	Drug	Human	I	-	-	-	-	[69]
Emond	2016	Env	Human	J	y	n	n	animal *in vivo*	[130]
Strikwold	2017	Env	Rat	J	y	n	n	animal *in vivo*/*in vitro*	[87]

y = yes; **n** = no; **Subst.nature** = substance nature; **Sym** = symmetrical; **fBW** = proportional to fetal bodyweight; **mBW =** proportional to maternal bodyweight; **Source** = source of information; **fBF =** fetal blood flow to placenta. *For Trichloroacetic acid (TCA). **The considered passive diffusion parameter is set between placenta and fetus in Emond et al. and between placenta and fetal plasma in Clewell et al.

Table 3: Placental active transport parameterization in gestational pPBPK models.

First author	Year	Species	Class	Active transport				Comments, reference
				Dir	Sym	fBW	mBW	
Clewell	2003	Rat	C	m → f	n	n	y (V_{max})	Perchlorate: Km obtained from thyroid slices data, [146] Iodide: Km obtained from sheep thyroid slices data, [147] Vmax source unknown
Clewell	2007	Human	K	m → f	n	n	y (V_{max})	Km and Vmax were set to rat value in absence of human data
Sweeney	2009	Rat, rabbit, human	D	m → f	n	n	y (V_{max})	Human Km obtained from thyroid slices data, [146] Human Vmax estimated from pregnant rat data of iodide uptake in other tissues
Yoon	2011	Rat, human	D	m → f	n	y (V_{max})	n	Parameters were varied until the active transfer became more than 95% of the flux to the fetal side
Lumen	2013	Human	E	m → f	n	n	y (V_{max})	Km obtained from thyroid slices data, [146] Values of Vmax were fitted during model calibration
Zhang	2017	Human	C	m → f & f → m	n	n	n	Set to zero before quantitative proteomic data

y = yes; **n** = no; **Dir** = direction; **Sym** = symmetrical; **fBW** = proportional to fetal bodyweight; **mBW** = proportional to maternal bodyweight; **Source** = source of information. **m → f** = maternal to fetal. **f → m** = fetal to maternal.

Highlights

- We reviewed pregnancy PBPK models according to the modeling of placental transfers
- Various placental sub-models were identified in the 50 original pPBPK models
- Model simulations showed the influence of placental transfers on fetal exposures
- We propose a new structure that integrates two placental vascularization steps
- *In silico* and experimental methods providing quantitative transfer data are shown

Supplemental Material

Placental transfer of xenobiotics in animal and human physiologically based pharmacokinetic models of pregnancy

Marc Codaccioni, Frédéric Bois, Céline Brochot[1]

[1]**Correspondence:** Céline Brochot; celine.brochot@ineris.fr

Group 1 equations

In the following equations, F_{mat} and F_{fet} represent respectively the maternal and the fetal blood flows to the placenta expressed in $[v].[t]^{-1}$, C_x (with x suffix corresponding to a compartment) refers to the internal compartmental chemical concentration expressed in $[m].[v]$, Q_x (with x suffix corresponding to a compartment) represents the quantity of substance in a specific compartment, expressed in $[m]$, K_{xy} (with x and y corresponding to two different compartments) refers to the apparent diffusional transfer constant expressed in $[v].[t]^{-1}$ and $PC_{xt:b}$ (with x suffix corresponding to a compartment) is the placental tissue to blood partition coefficient.

The mb, fb, mp, mpb, p, fpb and fp refer to maternal blood, fetal blood, maternal placental tissue, maternal placental blood, placental tissue, fetal placental blood and fetal placental tissue compartments respectively.

Class A model:

$$\frac{dQ_{mp}}{dt} = K_{mpb,mp} \times \left(C_{mpb} - \frac{C_{mp}}{PC_{mp_{t:b}}}\right)$$

$$\frac{dQ_{mpb}}{dt} = F_{mat} \times \left(\frac{C_{maternalPBPK}}{PC_{maternalPBPK_{t:b}}} - C_{mpb}\right) - \frac{dQ_{mp}}{dt} - transfer_{mpb:fpb}$$

$$\frac{dQ_{fpb}}{dt} = F_{fet} \times \left(\frac{C_{fetalPBPK}}{PC_{fetalPBPK_{t:b}}} - C_{fpb}\right) - \frac{dQ_{fp}}{dt} + transfer_{mpb:fpb}$$

$$\frac{dQ_{fp}}{dt} = K_{fpb,fp} \times (C_{fpb} - \frac{C_{fp}}{PC_{fp_{t:b}}})$$

$$transfer_{mpb:fpb} = K_{mpb,fpb} \times (C_{mpb} - C_{fpb})$$

Parameterization of apparent diffusional transfer constants from Gray et al. (1995) is:

$$K_{mpb,mp} = k_{pla} \times V_{mpb}$$

$$K_{fpb,fp} = k_{pla} \times V_{fpb}$$

$$K_{mpb,fpb} = k_{mfpla} \times V_{mpb}$$

Where k_{pla} and k_{mfpla} parameters are transfer rate, constants expressed in $[t]^{-1}$, and V_x (with x suffix corresponding to a compartment) refers to the compartmental volume, expressed in $[v]$.

Class B model:

$$\frac{dQ_{mp}}{dt} = K_{mp,mpb} \times \left(C_{mpb} - \frac{C_{mp}}{PC_{mp_{t:b}}}\right)$$

$$\frac{dQ_{mpb}}{dt} = F_{mat} \times \left(\frac{C_{maternalPBPK}}{PC_{maternalPBPK_{t:b}}} - C_{mpb}\right) - \frac{dQ_{mp}}{dt} - transfer_{mpb,fp}$$

$$\frac{dQ_{fp}}{dt} = transfer_{mpb:fp} - transfer_{fp:fpb}$$

$$\frac{dQ_{fpb}}{dt} = F_{fet} \times \left(\frac{C_{fetalPBPK}}{PC_{fetalPBPK_{t:b}}} - C_{fpb}\right) + tranfer_{fp:fpb}$$

$$transfer_{mpb:fp} = K_{mpb,fp} \times (C_{mpb} - \frac{C_{fp}}{PC_{fp_{t:b}}})$$

$$transfer_{fp:fpb} = K_{fp,fpb} \times (\frac{C_{fp}}{PC_{fp_{t:b}}} - C_{fpb})$$

$P_{mp,mpb}$, $P_{mpb,fp}$ and $P_{fp,fpb}$ refer to the substance permeabilities in $[l].[t]^{-1}$ ($[l]$ stands for length) and are computed according to Dallmann et al. (2017):

$$K_{mp,mpb} = P_{mp,mpb} \times SA$$

$$K_{mpb,fp} = P_{mpb,fp} \times SA$$

$$K_{fp,fpb} = P_{fp,fpb} \times SA$$

$$P_{mp,mpb} = P_{mpb,fp} = P_{fp,fpb} = \left(\frac{MWeff}{336}\right)^{-6} \times \frac{10^{logMA}}{5} \times 10^{-6}$$

Where SA represents the materno-fetal surface of exchange in $[l]^2$, MWeff and logMA are respectively the effective molecular weight of a substance and the logarithm of its affinity to membranes.

Class C model:

$$\frac{dQ_{mpb}}{dt} = F_{mat} \times \left(\frac{C_{maternalPBPK}}{PC_{maternalPBPK_{t:b}}} - C_{mpb}\right) - transfer_{mpb:p}$$

$$\frac{dQ_p}{dt} = transfer_{mpb:p} - transfer_{p:fb}$$

$$\frac{dQ_{fb}}{dt} = F_{fet} \times \left(\frac{C_{fetalPBPK}}{PC_{fetalPBPK_{t:b}}} - C_{fb}\right) - transfer_{fb:p}$$

$$transfer_{mpb:p} = K_{mpb,p} \times (C_{mpb} - \frac{C_p}{PC_{p_{t:b}}})$$

$$transfer_{p:fb} = K_{p,fb} \times (\frac{C_p}{PC_{p_{t:b}}} - C_{fb})$$

$$transfer_{fpb:p} = K_{fb,p} \times (\frac{C_p}{PC_{p_{t:b}}} - C_{fb})$$

The calculation of $K_{mpb,p}$, $K_{p,fb}$ and $K_{fb,p}$ is based on Clewell et al. (2003). $K_{p,fb}$ and $K_{fb,p}$ are set to different values to consider an asymmetrical materno-fetal exchange of the chemical.

$$K_{mpb,p} = PAPc \times BW_{fetal}^{0.75}$$

$$K_{p,fb} = Cltransc_{p,fb} \times BW_{fetal}^{0.75}$$

$$K_{fb,p} = Cltransc_{fb,p} \times BW_{fetal}^{0.75}$$

Where *PAPc* is the permeability surface area exchange in $[v].[t]^{-1}.[m]^{-1}$ between the maternal placental blood and the placental tissue, $Cltransc_{p,fb}$ and $Cltransc_{fb,p}$ are the asymmetrical clearances occurring between the placental tissue and the fetal placental blood, expressed in $[v].[t]^{-1}.[m]^{-1}$.

Class D model:

$$\frac{dQ_p}{dt} = F_{mat} \times \left(\frac{C_{maternalPBPK}}{PC_{maternalPBPK_{t:b}}} - \frac{C_p}{PC_{p_{t:b}}}\right) - transfer_{p:fb}$$

$$\frac{dQ_{fb}}{dt} = F_{fet} \times \left(\frac{C_{fetalPBPK}}{PC_{fetalPBPK_{t:b}}} - C_{fb} \right) - transfer_{fb:p}$$

$$transfer_{p:fb} = K_{p,fb} \times (\frac{C_p}{PC_{p_{t:b}}} - C_{fb})$$

$$transfer_{fb:p} = K_{fb,p} \times (\frac{C_p}{PC_{p_{t:b}}} - C_{fb})$$

For $K_{p,fb}$ and $K_{fb,p}$, Martinez et al. (2017), for example, used clearances used in animals.

Class E model:

$$\frac{dQ_{mpb}}{dt} = F_{mat} \times \left(\frac{C_{maternalPBPK}}{PC_{maternalPBPK_{t:b}}} - C_{mpb} \right) - transfer_{mpb:p}$$

$$\frac{dQ_p}{dt} = F_{fet} \times \left(\frac{C_{fetalPBPK}}{PC_{fetalPBPK_{t:b}}} - \frac{C_p}{PC_{p_{t:b}}} \right) + transfer_{mpb:p}$$

$$transfer_{mpb:p} = K_{mpb,p} \times (C_{mpb} - \frac{C_p}{PC_{p_{t:b}}})$$

$K_{mpb,p}$ setting corresponds to the methodology found in Lumen et al. (2013):

$$K_{mpb,p} = PAC \times BW_{fetal}^{0.75}$$

Where PAC is the permeability surface area exchange in $[v].[t]^{-1}.[m]^{-1}$ between the maternal placental blood and the fetal placental tissue.

Class F model:

$$\frac{dQ_{mp}}{dt} = F_{mat} \times \left(\frac{C_{maternalPBPK}}{PC_{maternalPBPK_{t:b}}} - \frac{C_{mp}}{PC_{mp_{t:b}}} \right) - transfer_{mp:fp}$$

$$\frac{dQ_{fp}}{dt} = F_{fet} \times \left(\frac{C_{fetalPBPK}}{PC_{fetalPBPK_{t:b}}} - \frac{C_{fp}}{PC_{fp_{t:b}}} \right) + transfer_{mp:fp}$$

$$transfer_{mp:fp} = K_{mp,fp} \times (C_{mp} - C_{fp})$$

$K_{mp,fp}$ calculation is based on De Sousa Mendes. (2015):

$$K_{mp,fp} = Dcot \times \frac{Vpl}{Vcot}$$

Where Dcot stands for the *ex vivo* diffusion parameter measured in a cotyledon. *Vpl* and *Vcot* refer to the placental volume and the cotyledon volume respectively.

Class G model:

$$\frac{dQ_{mb}}{dt} = F_{mat} \times \left(\frac{C_{maternalPBPK}}{PC_{maternalPBPK_{t:b}}} - C_{mb} \right) - transfer_{mb:fb}$$

$$\frac{dQ_{fb}}{dt} = F_{fet} \times \left(\frac{C_{fetalPBPK}}{PC_{fetalPBPK_{t:b}}} - C_{fb} \right) - transfer_{fb:mb}$$

$$transfer_{mb:fb} = K_{mb,fb} \times \left(C_{mb} - C_{fb} \right)$$

$$transfer_{fb:mb} = K_{fpb,mpb} \times \left(C_{fb} - C_{mb} \right)$$

In Schalkwijk et al. (2017) $K_{mb,fb}$ is parameterized by a maternal blood to fetal blood clearance (Cl_{mf}) and $K_{fb,mb}$ a fetal blood to maternal blood clearance (Cl_{fm}).

Class H model:

$$\frac{dQ_p}{dt} = F_{mat} \times \frac{C_{maternalPBPK}}{PC_{maternalPBPK_{t:b}}} + F_{fet} \times \frac{C_{fetalPBPK}}{PC_{fetalPBPK_{t:b}}} - (F_{mat} + F_{fet}) \times \frac{C_p}{PC_{p_{t:b}}}$$

The double blood flow limited design of the placenta compartment implies that there is no need for transfer constant for exchange between maternal and fetal blood. Kim et al. (1996) used this structure for a rabbit p-PBTK model.

Group 2 equations

In the following equations, F_{mat} represents the maternal blood flow to the placenta expressed in $[v].[t]^{-1}$, C_x (with x suffix corresponding to a compartment) refers to the internal compartmental chemical concentration expressed in $[m].[v]^{-1}$, Q_x (with x suffix corresponding to a compartment) represents the amount of substance in a specific compartment expressed in $[m]$, K_{xy} (with x and y corresponding to two different compartments) refers to the apparent diffusional transfer constants expressed in $[v].[t]^{-1}$ and $PC_{xt:b}$ (with x suffix corresponding to a compartment) is the placental tissue to blood partition coefficient between tissue and blood.

The fetoplacentalunit, p, pb, f and fb refer to the fetoplacental unit, placenta, placental blood, fetus and fetal blood compartments respectively.

Class I model:

$$\frac{dQ_{fetoplacentalunit}}{dt} = F_{mat} \times (\frac{C_{maternalPBPK}}{PC_{maternalPBPK_{t:b}}} - \frac{C_{fetoplacentalunit}}{\mathrm{PC}_{\mathrm{fetoplacentalunit_{t:b}}}})$$

Class J model:

J1 $$\frac{dQ_p}{dt} = F_{mat} \times \left(\frac{C_{maternalPBPK}}{PC_{maternalPBPK_{t:b}}} - \frac{C_p}{PC_{p_{t:b}}}\right) - K_{p,f} \times (C_p - C_f)$$

J2 $$\frac{dQ_p}{dt} = F_{mat} \times \left(\frac{C_{maternalPBPK}}{PC_{maternalPBPK_{t:b}}} - \mathrm{C}_p\right) - K_{p,f} \times (C_p - \frac{C_f}{PC_{f_{t:b}}})$$

J3 $$\frac{dQ_p}{dt} = F_{mat} \times \left(\frac{C_{maternalPBPK}}{PC_{maternalPBPK_{t:b}}} - \frac{C_p}{PC_{p_{t:b}}}\right) - K_{p,f} \times (\frac{C_p}{PC_{p_{t:b}}} - \frac{C_f}{PC_{f_{t:b}}})$$

J4 $$\frac{dQ_p}{dt} = F_{mat} \times \left(\frac{C_{maternalPBPK}}{PC_{maternalPBPK_{t:b}}} - \frac{C_p}{PC_{p_{t:b}}}\right) - K_{p,f} \times (C_p - \frac{C_f}{PC_{f_{t:b}}})$$

Class K model:

$$\frac{dQ_{pb}}{dt} = F_{mat} \times \left(\frac{C_{maternalPBPK}}{PC_{maternalPBPK_{t:b}}} - C_{pb}\right) - transfer_{pb:p}$$

$$\frac{dQ_p}{dt} = transfer_{pb:p} - transfer_{p:fb}$$

$$\frac{dQ_{fb}}{dt} = transfer_{p:fb}$$

$$tansfer_{pb:p} = K_{pb,p} \times (C_{pb} - \frac{Cp}{PC_{p_{t:b}}})$$

$$transfer_{p:fb} = K_{p,fb} \times (\frac{Cp}{PC_{p_{t:b}}} - C_{fb})$$

Class L model:

$$\frac{dQ_{pb}}{dt} = F_{mat} \times \left(\frac{C_{maternalPBPK}}{PC_{maternalPBPK_{t:b}}} - C_{pb}\right) - transfer_{pb:p}$$

$$\frac{dQ_p}{dt} = transfer_{pb:p} - transfer_{p:f}$$

$$\frac{dQ_f}{dt} = transfer_{p:f}$$

$$transfer_{pb:p} = K_{pb,p} \times \left(C_{pb} - \frac{C_p}{PC_{p_{t:b}}} \right)$$

$$transfer_{p:f} = K_{p,f} \times \left(C_p - C_f / PC_{f_{t:b}} \right)$$

Class P model equations

In the following equations, F_{mat} represents the maternal blood flow to the placenta expressed in $[v].[t]^{-1}$, C_x (with x suffix corresponding to a compartment) refers to the internal compartmental chemical concentration expressed in $[m].[v]^{-1}$, Q_x (with x suffix corresponding to a compartment) represents the amount of substance in a specific compartment expressed in $[m]$, K_{xy} (with x and y corresponding to two different compartments) refers to the apparent diffusional transfer constants expressed in $[v].[t]^{-1}$ and $PC_{xt:b}$ (with x suffix corresponding to a compartment) is the placental tissue to blood partition coefficient between tissue and blood.

The mp, ivs and fp refer to maternal placenta, intervillous space and fetal placenta compartments respectively.

$$\frac{dQ_{PBPKmat}}{dt} = F_{mat} \times \left(\frac{C_{mp}}{PC_{mp_{t:b}}} - \frac{C_{maternalPBPK}}{PC_{maternalPBPK_{t:b}}} \right)$$

$$\frac{dQ_{mp}}{dt} = F_{mat} \times \left(\frac{C_{maternalPBPK}}{PC_{maternalPBPK_{t:b}}} - \frac{C_{mp}}{PC_{mp_{t:b}}} \right) - transfer_{mp:ivs}$$

$$\frac{dQ_{ivs}}{dt} = transfer_{mp:ivs} - transfer_{ivs:fp}$$

$$\frac{dQ_{fp}}{dt} = F_{fet} \times \left(\frac{C_{fetalPBPK}}{PC_{fetalPBPK_{t:b}}} - \frac{C_{fp}}{PC_{fp_{t:b}}} \right) + transfer_{ivs:fp}$$

$$\frac{dQ_{PBPKfet}}{dt} = F_{fet} \times \left(\frac{C_{fp}}{PC_{fp_{t:b}}} - \frac{C_{fetalPBPK}}{PC_{fetalPBPK_{t:b}}} \right)$$

$$transfer_{mp:ivs} = K_{mp,ivs} \times \left(\frac{C_{mp}}{PC_{mp_{t:b}}} - C_{ivs} \right)$$

$$transfer_{ivs:fp} = K_{ivs,fp} \times \left(C_{ivs} - \frac{C_{fp}}{PC_{fp_{t:b}}} \right)$$

Exposure scenario

A single dose of 0.6 mg of a theorical substance is administrated orally.

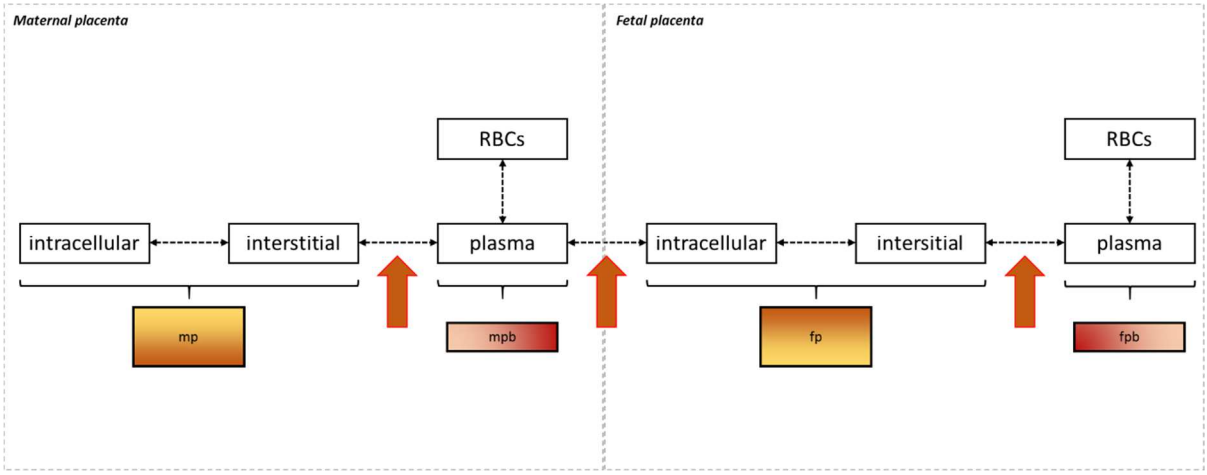

Figure S1: Dallmann et al. representation of placental transfer. Orange arrows show the three diffusional transfer parameters considered in our classification.

Table S1: Parameterization of partition coefficients (PC, unitless) for group 1 & 2 models simulations.

Class / Comp	A	B	C	D	E	F	G	H	I	J1	J2	J3	J4	K	L
PBPKmat	10	10	10	10	10	10	10	10	10	10	10	10	10	10	10
mp	3	3	-	-	-	3	-	-	-	-	-	-	-	-	-
mpb	-	-	-	-	-	-	-	-	-	-	-	-	-	-	-
p	-	-	3	3	3	-	-	3	-	3	3	3	3	3	3
fpb	-	-	-	-	-	-	-	-	-	-	-	-	-	-	-
fp	3	3	-	-	-	3	-	-	-	-	-	-	-	-	-
Fetoplacental unit	-	-	-	-	-	-	-	-	-	-	-	-	-	-	-
f	-	-	-	-	-	-	-	-	-	-	-	8	8	-	8
PBPKfet	8	8	8	8	8	8	8	8	8	-	-	-	-	-	-

Table S2: Parameterization of volumes (Vol, in L) for group 1 & 2 models simulations.

Class / Comp	A	B	C	D	E	F	G	H	I	J1	J2	J3	J4	K	L
PBPKmat	65	65	65	65	65	65	60	65	65	65	65	65	65	65	65
mp	0.12	0.12	-	-	-	0.37	-	-	-	-	-	-	-	-	-
mpb	0.25	0.25	0.25	-	0.25	-	-	-	-	-	-	-	-	-	-
mb	-	-	-	-	-	-	5	-	-	-	-	-	-	-	-
p	-	-	0.46	0.71	0.46	-	-	0.71	-	0.71	0.71	0.71	0.71	0.4	0.4
pb	-	-	-	-	-	-	-	-	-	-	-	-	-	0.31	0.31
fpb	0.06	0.06	-	-	-	-	-	-	-	-	-	-	-	-	-
fp	0.28	0.28	-	-	-	0.34	-	-	-	-	-	-	-	-	-
fb	-	-	0.25	0.25	-	-	0.25	-	-	-	-	-	-	0.25	-
Fetoplacental unit	-	-	-	-	-	-	-	-	3.71	-	-	-	-	-	-
f	-	-	-	-	-	-	-	-	-	3	3	3	3	-	3
PBPKfet	3	3	2.75	2.75	3	3	2.75	3	-	-	-	-	-	-	-

Table S3: Time to reach steady-state in fetal compartment in group 2 models. Fetal compartment corresponds to *Fetoplacental unit* in class I models, *fb* in class K models and *f* in J and L models.

Time to reach steady-state	Placental transfer structure classes
Instantaneously	I
< 40 hours	J1, K
≈ 180 hours	J2, J3, J4
> 400 hours	L

Table S4: Parameterization of volumes (Vol, in L) and partition coefficients (PC, unitless) for P model simulations.

Comp	Vol	PC
Maternal PBPK	65	10
mp	0.12	3
ivs	0.31	-
fp	0.28	3
Fetal PBPK	3	8

Class B model GNU MCSim code:

"transferB.in" file:

```
Integrate (Lsodes, 1e-12, 1e-12, 1);
OutputFile("transferB_ss.out");
  inf = 0;
  dose = 0.6;
  PC_PBPKmat = 10;
  PC_mp = 3;
  PC_fp = 3;
  PC_PBPKfet = 8;
  F_mat = 45;
  F_fet = 30;
  V_PBPKmat = 65;
  V_mp = 0.12;
  V_mpb = 0.25;
  V_fpb = 0.06;
  V_fp = 0.28;
  V_PBPKfet = 3;
  K_mp_mpb = 1;
  K_mpb_fp = 1;
  K_fp_fpb = 1;

Experiment {
  StartTime (0);
PrintStep(Q_check, C_PBPKmat, C_mp, C_mpb, C_fpb, C_fp, C_PBPKfet, 0, 2400, 0.1);
}
End.
```

"transferB.model" file:

```
States = {
  Q_inf,
  Q_PBPKmat,
  Q_mp,
  Q_mpb,
  Q_fpb,
```

```
  Q_fp,
  Q_PBPKfet
}; # End of States

Outputs = {
  C_PBPKmat,
  C_mp,
  C_mpb,
  C_fpb,
  C_fp,
  C_PBPKfet,
  Q_check,
  Q_placenta
}; # End of Outputs

  #~~~~~# PARAMETERS #~~~~~#
  inf;
  dose;
  PC_PBPKmat;
  PC_mp;
  PC_fp;
  PC_PBPKfet;
  F_mat;
  F_fet;
  V_PBPKmat;
  V_mp;
  V_mpb;
  V_fpb;
  V_fp;
  V_PBPKfet;
  K_mp_mpb;
  K_mpb_fp;
  K_fp_fpb;

Initialize {
```

```
  Q_PBPKmat = dose;
}; # End of model initialization


Dynamics {
  C_PBPKmat = Q_PBPKmat / V_PBPKmat;
  C_mp = Q_mp / V_mp;
  C_mpb = Q_mpb / V_mpb;
  C_fpb = Q_fpb / V_fpb;
  C_fp = Q_fp / V_fp;
  C_PBPKfet = Q_PBPKfet / V_PBPKfet;
  #~~~~~# STRUCTURE #~~~~~#
  dt(Q_inf) = inf;
  transfer_mpb_fp = K_mpb_fp * (C_mpb - (C_fp/PC_fp));
  transfer_fp_fpb = K_fp_fpb * ((C_fp/PC_fp) - C_fpb);
  dt(Q_PBPKmat) = dt(Q_inf) + F_mat * (C_mpb - (C_PBPKmat/PC_PBPKmat));
  dt(Q_mp) = K_mp_mpb * (C_mpb - (C_mp/PC_mp));
  dt(Q_mpb) = F_mat * ((C_PBPKmat/PC_PBPKmat) - C_mpb) - dt(Q_mp) -
transfer_mpb_fp;
  dt(Q_fpb) = F_fet * ((C_PBPKfet/PC_PBPKfet) - C_fpb) + transfer_fp_fpb;
  dt(Q_fp) = transfer_mpb_fp - transfer_fp_fpb;
  dt(Q_PBPKfet) = F_fet * (C_fpb - (C_PBPKfet/PC_PBPKfet));
}; # End of Dynamics


CalcOutputs {
  Q_placenta = Q_mp + Q_mpb + Q_fpb + Q_fp;
  Q_check = (Q_inf + dose) - (Q_PBPKmat + Q_PBPKfet + Q_placenta);
} # End of CalcOutputs
End.
```